Climate- and Human- Induced Land Cover Change and its Effects on the Permafrost System in the Lower Yenisei River of the Russian Arctic

by Kelsey Elizabeth Nyland

B.A. Geography, Environmental Studies, May 2013, The George Washington University

A Thesis submitted to

The Faculty of
The Columbian College of Arts and Sciences
of The George Washington University
in partial fulfillment of the requirements
for the degree of Masters of Arts

May 17, 2015

Thesis directed by

Nikolay I. Shiklomanov
Associate Professor of Geography

© Copyright 2015 by Kelsey Elizabeth Nyland
All Rights Reserved

Acknowledgments

The author wishes to thank her advisor, Dr. Nikolay Shiklomanov, for his mentorship. The author also wishes to than additional thesis committee members, Drs. Dmitry Streletskiy, Ryan Engstrom, and Timothy Heleniak, for their expertise and guidance in designing and performing this research. In addition, Dr. Streletskiy, in collaboration with Moscow State University's Dr. Valery Grebenets, organized the International Permafrost Field Course, and allowed her to participate in multiple field seasons in the Lower Yenisei river region. While in the field, Dr. Nikita Tananaev, head of the Igarka Geocryological Laboratory, was of great assistance, providing historical photos, and assisting with local logistics. Technical assistance was provided by Dr. Michael Mann with R Statistical Language and Richard Hinton with ArcGIS and cartography. Dr. Alexander Shiklomanov and Stanley Glidden from the University of New Hampshire also helped to obtain NASA Modern Era-Retrospective Analysis data for the study area, critical to the analysis of land cover changes found in this work. Lastly, she would like to thank her fellow Research Assistant, Avery Sandborn, for her support and friendship throughout the Master's degree program.

Funding for this thesis research was provided by NSF-Grants ARC-1204110, PLR-1304555, and PLR-1231294, Research Council of Norway project 220613, and The George Washington University's Geography Department, Campbell Summer Research Grant.

Abstract of Thesis

Climate- and Human- Induced Land Cover Change and its Effects on the Permafrost System in the Lower Yenisei River of the Russian Arctic

Climate warming is occurring at an unprecedented rate in the Arctic, seriously impacting sensitive environments, and triggering land cover change. These changes are compounded by localized human influences. This work classifies land cover change for the Lower Yenisei River, identifies those changes that were climate- and anthropogenic-induced, and discusses the implications for the underlying permafrost system. This is accomplished using a modified version of the "Landsat dense time stacking" methodology for three time periods spanning 29 years that are representative of Russian socio-economic transitions during the mid- to late-1980s (1985-1987), the early 2000s (2000-2002), and the contemporary 2010s (2012-2014). The classified area includes three cities indicative of different post-Soviet socio-economic situations, including continued population and infrastructure decline (Igarka), a relatively stable community (Dudinka), and a community receiving local reinvestment (Norilsk). The land cover classification, in tandem with regional climate reanalysis data, enabled climate- and anthropogenic- induced changes to be identified, characterized, and quantified. Climatic changes within the natural environments have produced a steady greening effect throughout the study area, as well as an increase in large lake abundance, indicative of permafrost degradation. Pollution, in close proximity to heavy industrial activity, caused a secondary plant succession process. The results of this work provide both map products that can be applied to future research in this region, as well as insights into the impacts of the warming climate and human presence on sensitive Arctic environments.

Table of Contents

Acknowledgments iii
Abstract of Thesis iv
Table of Contents v
List of Figures vi
List of Tables viii
List of Equations ix
Chapter 1: Introduction 1
Chapter 2: Background to the Problem 4
Chapter 3: Hypotheses and Objectives 14
Chapter 4: Study Area 16
Chapter 5: Methodology 23
Chapter 6: Results and Discussion 35
Chapter 7: Conclusions 72
References 77

List of Figures

Figure 4.1: Study area map ……. 17

Figure 4.2: Permafrost distribution map …….. 19

Figure 4.3: Population change in Igarka, Dudinka, and Norilsk ……. 21

Figure 5.1: Classification model work flow diagram …….. 26

Figure 5.2: Photos of classified land covers …… 29

Figure 6.1: Classified time series maps ……..…. 38

Figure 6.2: Graph of land cover proportions ……...…… 40

Figure 6.3: Panel graphic of 5-year mean annual air temperatures ……. 42

Figure 6.4: Panel graphic of 5-year mean total annual precipitation ……..…. 43

Figure 6.5: Panel graphic of 5-year maximum annual snow depths ……...……. 44

Figure 6.6: Historical climate data from Igarka and Norilsk weather stations ……..... 46

Figure 6.7: Map series of surface hydrology change …….…….. 48

Figure 6.8: Graph of total lake area and number change ……...….. 49

Figure 6.9: Natural lake change examples in Landsat imagery ……...… 50

Figure 6.10: Map series of tundra and open forest change ……..… 52

Figure 6.11: Map series of closed forest change ……...…….…. 53

Figure 6.12: Map series of barren ground change ……...…… 54

Figure 6.13: Map series of built up area change …….……. 57

Figure 6.14: Time lapse photography of urban decline in Igarka ……..…….…. 58

Figure 6.15: Case study map series …….…. 61

Figure 6.16: Graphs of land cover proportions for each case study ……..... 63

Figure 6.17: Graph of total annual airborne emissions from Norilsk ……..…… 65

Figure 6.18: Industrial lake change examples in Landsat imagery …….. 68

List of Tables

Table 5.1: Classification model conditionals ……...… 27

Table 6.1: Classification accuracy confusion matrices …… 39

List of Equations

Equation 5.1: Normalized Difference Vegetation Index ……...…….. 26

Equation 5.2: Multinomial sample size ……... 30

Equation 5.3: Overall accuracy ……..... 32

Equation 5.4: Kappa coefficient …….. 32

Equation 5.5: User's accuracy …….…… 32

Equation 5.6: Producer's accuracy ……...… 32

Chapter 1: Introduction

There are multiple drivers of land cover change within contemporary Arctic environments, namely the warming climate and land cover changes which are exacerbated in areas of anthropogenic activity particularly where there is changing land use. These two drivers coincide and compound land cover changes in and around areas of anthropogenic activity. These changes have important implications for the surface energy balance and atmospheric feedback mechanisms, which in turn have significant impacts on Arctic residents and their activities (e.g. Gutman & Reissel 2010, Schneider von Deimling et al. 2012, Groisman et al. 2012, Hinzman et al. 2013, IPCC 2013).

Land cover changes surrounding urban and industrialized areas are some of the most drastic and also the most vulnerable to continued change (Gutman & Reissel 2010, Groisman et al. 2012). Many postulate that the ameliorating effects of warming atmospheric temperatures in the Arctic, causing sea ice to thin and reduce in extent, will open up shipping routes (Smith & Stephenson, 2013) and therefore the potential for further development (e.g. ACIA 2004, Ho 2010, Zellen 2009). For example, in the Canadian Arctic, there is an anticipated growth of settlements in coastal regions primarily to support oil and gas exploration along the continental shelf, as well as support for increased use of the Northwest Passage (Khon et al. 2010). Iqualuit, the capital of Nunavut, Canada, is an example of a coastal community currently developing through centralization strategies (Webber, 2014). In Nuuk, Greenland, there are similar proposed plans for urbanization. Oil and gas explorations in Greenland have expanded in the hope of developing natural resources. However, contrary to the development policies in

Canada, in Greenland they are also pursuing industrialization through smelting locally mined minerals. For instance, aluminum companies are still scouting land and advocating for a smelter to be built in Nuuk (Sejersen, 2010). Since much of this urbanization is still in the planning stages there is the potential to craft it in a sustainable manner by learning from the impacts caused by past Arctic development.

Russia is unique within the Arctic in that it already contains relatively large industrialized urban centers compared to the primarily indigenous communities and extraction outposts typically found elsewhere, such as the Alaskan and Canadian Arctic. To illustrate, following a rough line of comparable latitude (70˚N) are the following communities and their populations as of 2013: Norilsk, Russia with 177,700 people, Dudinka, Russia, with 22,300, Barrow, Alaska with 4,373, Igloolik, Canada with 2,000, and Uummannaq, Greenland with 1,282 (RosStat 2015, US Census 2015, Bureau, Statistics Canada 2013, Statistics of Greenland 2013).

Unlike proposed urbanization elsewhere in the Arctic, in Russia there have been urbanized and heavily industrialized cities at high latitudes for more than 60 years (e.g. Hill & Gaddy 2003, Heleniak 2009). The intensive urbanization in the Russian Arctic is a product of former Soviet planned development policies, which promoted migration into the Arctic and labor force consolidation into few sparsely-distributed settlements. In order to support settlements built in an extremely remote and harsh environments, huge government subsidies were required (Hill & Gaddy, 2003). The Soviet Union's focus on development in the Arctic, regardless of cost or difficulty, has left a problematic legacy for the Russian Federation. As the Soviet political and economic systems crumbled, so did the support for industries sustaining these Arctic cities. Today the Russian Arctic

landscape is strewn with crumbling infrastructure surrounding isolated pockets of intensified urban development. Despite the vast out migrations and general abandonment of many settlements, there are a small number of urban centers that are growing due to development. This growth is caused by renewed investment in natural resource extraction industries (Anoklin 2014, Kryukova et al. 2015) followed by new influxes of people migrating from collapsing communities in surrounding areas (Heleniak, 2009). These socio-economic changes continue to inflict significant stress on the natural environment.

The advanced industrial state of the Russian Arctic provides a unique opportunity to test new methods for observing land cover changes as a result of climatic and human influence. This work examines both climatic- and anthropogenic- induced land cover changes in the Lower Yenisei River Region of Central Siberia from 1985 to 2014 using the Landsat dense time stacking methodology. Three maps were created to capture the results of key periods of socio-economic transitions in Russia beginning (1985 - 1987), middle (2000 - 2002), and the most recent time period (2012 – 2014). The lessons gained from this work have the potential to better inform Arctic development strategies and apply these lessons to more sustainable Arctic.

Chapter 2: Background to the Problem

2.1 Arctic Amplification of Climatic Changes

Climate change is significantly amplified in the Arctic (IPCC, 2013). This amplification is triggered by feedback mechanisms related primarily to the reductions in sea ice extent and snow cover, which are characterized by a high albedo. The replacement of snow and ice with open water and vegetation (lower albedos) for increasingly longer periods throughout the year facilitates more absorption of solar radiation that heats the surface. This albedo-temperature feedback mechanism is one of the many reasons that it is important to study Arctic land cover changes as it exerts significant stress on these cold environments that are particularly sensitive to warming (Screen & Simmonds 2010, Bekryaev et al. 2010, Hinzman et al. 2013).

During the 20th century average air temperatures in the Arctic have increased by nearly twice the global average rate (IPCC 2013). This drastic warming in the Arctic has had numerous effects on the physical environment, including exacerbating sea ice loss (e.g. Screen & Simmonds 2010, Screen et al. 2013), warming and thawing of the permafrost (perennially frozen ground) (e.g. Pavlov 2006, Romanovsky et al. 2010, Fedorov et al. 2014), and the northward expansion of larger vegetation types (e.g. Jia et al. 2003, Sturm et al. 2005, Tape et al. 2006, Walker et al. 2011). All of these changes are connected through various feedback mechanisms that have the potential to positively or negatively impact the climate at the global scale (e.g. Screen and Simmonds 2010, Gutman & Reissell 2010, IPCC 2013).

Among the changes to land covers as a result of the warming climatic conditions, those that have already been altered by anthropogenic activities are considered to be more vulnerable to still further changes (Gutman & Reissell 2010, Groisman et al. 2012). The following is a review of previously observed natural and human system changes that have occurred in the Arctic, with a focus on the Russian Arctic.

2.2 Climatic Induced Impacts on Natural Systems

2.2.1 Impacts on Vegetation

Two distinct "greening" trends, or in other words the encroachment of taller vegetation species into new habitats, or changes in both the latitudinal and altitudinal treelines have been observed occurring in various Arctic regions (e.g. Lloyd 2005, Harsch et al. 2009). The latitudinal treeline is often depicted as a discrete line on maps, but the definition used to define this line varies. Traditionally, the boundary is based on the furthest extent of trees that reach two to three meters in height, but it has also been defined as the northernmost latitude or highest elevation of individual tree occurrences (Harsch et al., 2009). Shifts in both the latitudinal and altitudinal treelines, northward and upward respectively, have been documented in a number of *in situ* studies throughout the Arctic, including the Polar Urals (Shiyatov et al., 2005), the eastern portion of the Taymir Peninsula (Kharuk et al., 2006), and in Alaska (Lloyd, 2005). The increasing length of the growing season, thickening of the active layer (the uppermost soil layer that seasonally thaws), and increased snow are the primary factors that have been cited facilitating these shifts in the spatial extent of larger plant species in the Arctic. These changes have promoted increased growth, greater access to liquid water and nutrients,

and protection for taller plants from the extreme winter temperatures and abrasion from wind-blown particles (e.g. Forbes et al., 2010, Hallinger et al. 2010, Blok et al., 2011, Meyers-Smith et al. 2011).

The expansion of larger shrubs and trees in the Arctic significantly lowers the surface cover's albedo increasing regional heat absorption contributing to warmer near surface air temperatures. However, monitoring such changes in vegetation's albedo over recent decades has been found to have a negligible impact on summer air temperatures compared to the albedo effects from a longer snow free period (Chapin et al. 2005). Despite being a slower change to occur over time, the greening trends (tundra to shrub to forest conversions) are expected to continue and will eventually play a more significant role in the albedo feedback mechanism (Hinzman et al. 2013). In the meantime, vegetation plays a significant role as a thermal insulator for the ground thermal regime and changes in species complexes has significant implications for the degree to which atmospheric signals can impact ground temperatures.

2.2.2 Impacts on the Permafrost System

Permafrost is defined as any earth material that remains frozen (below $0^{\circ}C$) for two or more years (Williams & Smith 1989, French 2007, Muller 2008). Two geographic conditions facilitate the mean annual air temperatures necessary to form and maintain frozen ground: high latitudes or polar regions (latitudinal or polar permafrost) and high altitude regions (altitudinal permafrost). The upper most soil layer throughout permafrost affected areas that thaws seasonally is called the active layer (Williams & Smith, 1989).

Permafrost zonation is based on spatial continuity, and is generally referred to as follows: continuous, discontinuous (separated by taliks or unfrozen ground), sporadic (occasional patches of unfrozen ground), and isolated (permafrost that is spatially rare in occurrence such as at high elevations in low latitudes). However, these zonal definitions and the precise percentages of area occupied by permafrost within each zone can vary (French, 2007).

Significant portions of the Russian Arctic have undergone widespread ground warming and a northern retreat of the southern continuous permafrost boundary. This trend is projected to continue at an increasing rate for specific landscapes throughout Western Siberia (Pavlov 2006, Romanovsky et al. 2010, Fedorov et al. 2014). In addition, cryogenic geomorphic processes are anticipated to increase in frequency and magnitude as air temperatures continue to rise. These processes include the development of thermokarst (subsidence due to ground thaw), thermal cracking, and mass wasting processes such as thaw slumps and active-layer detachment slides (French, 2007). Changes to frozen ground are significant to land cover change as it can seriously modify topography, hydrology, and vegetation conditions (IPCC, 2013).

2.2.3 Hydrologic Impacts

Another climate-induced impact widely documented change throughout the Arctic are changes in surface hydrology. Contemporary regional scale large lake appearances and disappearances have been related to permafrost degradation in West Siberia (Smith et al., 2005). Through the detection of changes to large waterbodies over roughly 30 years across different permafrost zones, they note that widespread lake reductions and

disappearances were occurring within discontinuous permafrost zones, and that lakes were forming and expanding within the continuous permafrost zone. Within the continuous zone, the increases in lake numbers and total area were found to be products of thermokarst processes, or ponding from subsidence-caused depressions filling with ground ice melt water (French, 2007). The overall trend of lake reductions was attributed to thawing of already thin permafrost forming a "through talik", which allows for surface water to drain effectively (Smith et al., 2005). This has been confirmed by a number of studies that combined remotely sensed and *in situ* data that also found that taliks provide significantly more ground water storage than frozen soils, which are impermeable. Taliks that grow to a sufficient capacity can then lead to the complete drainage of lakes (Yoshikawa & Hinzman 2003, Muskett & Romanovsky 2011, Karlsson et al. 2012, 2014).

2.3 Human System Dynamics

2.3.1 Urbanization and Deurbanization in the Russian Arctic

There have been Russian settlements including extraction outposts, trapping villages, and ports in Arctic Siberia since the territory was officially incorporated into the Russian Empire in the mid-17th century. However, it was not until the late-19th through the mid-20th century that there was intensive development and industrialization of these settlements. The Soviet Union's planned development policies established new and grew preexisting settlements across Siberia in order to exploit the natural resources to fuel the rapidly industrializing nation and a desire to utilize a Northern Sea Route for shipping (e.g. Shiklomanov 2005, Blinnikov 2011). This impressive and rapid development was

accomplished despite the harsh conditions and extreme distances through the establishment of GULAG camps followed by planned development of those settlements through the support of large government subsidies. This development scheme resulted in primarily monotowns, or single industry towns, dispersed throughout the region (e.g. Hill & Gaddy 2003, Heleniak 2009, Parente et al. 2012).

Despite the abundant supply of natural resources, the dissolution of the Soviet Union in the early 1990s led to the failure of many of these industrial centers as they were not viable in an open market economy. With the loss of the government subsidies that sustained many of these activities in many cases cities found themselves without their sole employer. The result was a massive migration out of many of these Arctic communities (e.g. Hill & Gaddy 2003, Heleniak 2009, Parente et al. 2012).

In recent years several distinct demographic trends have emerged for these communities. While some continue to precipitously decline and their infrastructure largely abandoned, others have stabilized, or even experienced slight population growth thanks to local reinvestment particularly from oil, gas, and mineral extraction and processing industries (Heleniak 2009, Anoklin 2014, Kryukova et al. 2015). This is particularly true of areas with extractive industries such as rare earth elements or hydro carbons such as the mineral extraction occurring in Central Siberia and the oil and gas industry in West Siberia.

2.3.2 Human Impacts on Land Covers

Different components of developed areas in the Arctic have been studied previously in order to determine their impact on the surrounding tundra environment. For

example, elevating infrastructure on gravel pads has been a long standing and effective construction method on permafrost utilized throughout the Arctic. Built up roads and pads, however, have been found to significantly affect surrounding vegetation and soil conditions due to the generation and distribution of dust from associated anthropogenic activity (e.g. Walker et al. 1987, Auerbach & Walker 1997, Meyers-Smith et al. 2006). In addition, these structures modify local geomorphic processes such as limiting water drainage and causing thermokarst (e.g. Streletskiy et al. 2012a, b, Shiklomanov & Streletskiy 2013). Another well-studied environmental impact is the heat island effect. This locally intensified warming is produced by the combination of concentrated infrastructure and anthropogenic activity. In the Arctic, the heat island effect not only has significant impacts on the microclimate but also the ground thermal regime, critical to infrastructures' structural stability (Klene et al., 2013).

The warming effects of built-up areas on the ground thermal regime constitutes the primary inhibitor to future development in the Arctic (Hinkel et al. 2003, Grebenets et al. 2012, Streletskiy et al. 2012a, b). The majority of structures in the Russian Arctic are built according to the passive principle, which promotes equilibrium between the permafrost thermal regime and infrastructure foundations (Streletskiy et al., 2012a, b). The structural integrity of these buildings is based on the sustained thermal equilibrium between the permafrost and a structure's foundations. However, the vast majority of structures in the Russian Arctic are relics of Soviet development, and were not designed to handle current and projected environmental changes.

Environmental disturbances, such as those discussed above and other human activities have been previously examined through integrative studies from local to

regional scales. However, the majority of these works have been focused on the Alaskan Arctic, Fennoscandia, and the Yamal Peninsula in the western Siberian Arctic (e.g. Høgda et al. 1995, Walker et al. 2009, 2011).

In the Fennoscandia region of the Russian Arctic, land cover change studies focus on the impacts of emissions from smelters in Nikel and Zapolyarnyy, on vegetation. These land cover change effects are not just an environmental concern but also a geopolitical one as, emissions cross international borders affecting Finland and Norway (e.g. Høgda et al. 1995, Tømmervik et al. 1995, AMAP 2010). Several studies from this region have concluded that there is a process of plant succession following initially pollution disturbance and the industrial barrens are eventually reclaimed by hardier native shrub and grass species including crow berries (*Empetrum nigrum* ssp.) (Bakkal 1992, Tømmervik 1995), bilberrys (*Vaccinium myrtillus*), and grasses (*Poa* ssp.) (Deyeva & Maznaya 1993, Tømmervik 1995).

In western Siberia where there is significant development in the oil and gas industries competing with reindeer herding and husbandry practices. In this region there has been substantial ecosystem change including areas undergoing fundamental shifts in vegetative complexes (Kumpaula et al., 2011). Cumulative effects of development on vegetation have been primarily monitored through simple vegetative indices such as the Normalized Difference Vegetation Index (NDVI) and *in situ* transect studies which have shown distinct 'greening' trends or healthier, greener vegetation. These results have also been compared to personal accounts from local indigenous peoples and land use development policies (Walker 2009, 2011). All of these works have been limited in some

way by data constraints particularly due to the availability and quality of remotely sensed imagery (e.g. Walker et al. 2009, 2011, Goetz et al. 2011, Kumpaula et al. 2011).

The Arctic is inherently remote and poses many logistical challenges to *in situ* research. Remote sensing presents a unique opportunity to complement traditional monitoring schemes. Classifying land covers from satellite imagery offers a less labor intensive way to attain data for a broader spatial coverage at more frequent time intervals. However, remote sensing in the Arctic is complicated by consistent cloud coverage, data gaps, and polar night. This work examined almost 30 years of land cover changes in the Lower Yenisei River region of Central Siberia with the method called Landsat dense time stacking that compensated for such data limitations. The area of interest in the Lower Yenisei includes three cities representative of diverse post-Soviet socio-economic trends.

2.4 Landsat TM Imagery Analysis and Application to Arctic Environments

Landsat imagery is a powerful remote sensing dataset in that it offers the longest record (1972 to present) of continuous and consistent data for the entire globe, and is freely processed and available for download through the US Geological Survey's Glovis website. From its beginnings, these data have been intended in part for the detection of urban development and its impacts on surrounding natural land covers (e.g. Friedman & Angelici 1979, Todd 1977). However, the use of satellite imagery is complicated in Arctic applications due to consistently high amounts of cloud cover, data gaps, high heterogeneous landscapes, and the small scale and dispersed nature of development (Kumpula et al. 2011, Stow et al. 2004, Wallace 2012).

Similar challenges for remote sensing based studies of urban development in other lower latitude regions have been successfully dealt with by utilizing dense time stacks of Landsat imagery. This methodology has been applied to a variety of spatial change studies including forestry (Kennedy et al., 2007) and tracking urban morphologies (Schneider, 2012) in lower latitude regions. By ignoring the established use of an anniversary date for change detection, this methodology includes scenes from all seasons, in addition to imagery normally rejected due to data gaps and high amounts of cloud cover. A time period is set and scenes stacked in the hope that areas obscured by cloud cover or data gaps might be compensated for by the coverage of another image within the stack. This "brute force" approach creates a more complete dataset and can incorporate additional spatial data such as elevation and calculated indices, for example the Normalized Difference Vegetation Index (NDVI) (Rouse et al., 1974). Stacking a number of images to compensate for suboptimal data and including ancillary spatial information allows for a more nuanced classification scheme to be developed (Kennedy et al. 2007, Schneider 2012).

This technique presents an opportunity to overcome the challenges posed by Arctic environments and a chance to better incorporate remote sensing into Arctic impact studies. For these reasons, dense time stacking was selected as the primary methodological technique for land cover classification in this work. In this capacity, this work not only utilized the technique to quantify the changes taking place in the Lower Yenisei, but it also provided an assessment of the general applicability of the time-stacking technique for land cover change analysis throughout the circum-Arctic region.

Chapter 3: Hypotheses and Objectives

Based on the literature and observed changes to Arctic land cover and the permafrost system the following hypotheses were formed:

1) Both climatic and anthropogenic forcings are acting on land covers in the Lower Yenisei River region; and the areas that they impact are distinct from those areas only impacted by climatic forcings.
2) Socio-economic factors trigger growth or decay of urban settlements in the Russian Arctic, putting significant stress on the surrounding environment. In the presence of climate change this can potentially intensify permafrost warming and degradation.

These hypotheses were tested and assessed via a series of related and successive objectives which are:

1) Test the Landsat dense time stacking methodology for its applicability and effectiveness for classifying Arctic land covers and detecting change.
2) Create a thematic map series using the developed classification methodology from the mid-1980s to 2014 for the Lower Yenisei River region including the cities of Igarka, Dudinka, and Norilsk.

3) Quantify the aerial extent of land cover changes that have occurred throughout the time series and identify possible drivers for these changes.
4) Quantify changes in large lake areas in both the continuous and discontinuous permafrost zones to characterize permafrost degradation.

The first of these objectives, creating a land cover map time series, is dependent on the development of a land cover classification methodology suitable for impact assessment in the Lower Yenisei River region. Such a methodology was developed based on classification techniques previously described in the literature review and various thresholds for dense spatial data stacks of Landsat imagery, digital elevation models (DEM), and other available data.

Chapter 4: Study Area

This work focuses on the lower Yenisei River region of the Central Siberian Arctic as covered by two adjacent Landsat scenes for an approximately 60,750 km^2 area (Figure 4.1). The Yenisei River contributes the largest annual discharge into the Arctic Ocean flowing north into the Kara Sea (Shiklomanov & Lammers, 2009). This major Eurasian river system separates two major physiographic regions of Siberia; the West Siberian Plane to the west, and the Central Siberian Plateau to the east including the Putorana Mountains and Plateau included within the study area. The study area has a subarctic climate, or Dfc, as classified by the Köppen climate classification system which entails fewer than four months per year with a mean temperature greater than 10°C, and a cold summer where the hottest month of the year's mean temperature is less than 22°C but greater than 10°C, the coldest month's mean temperature is below 0°C but greater than -38°C, and without a distinct dry season (Peel et al., 2007).

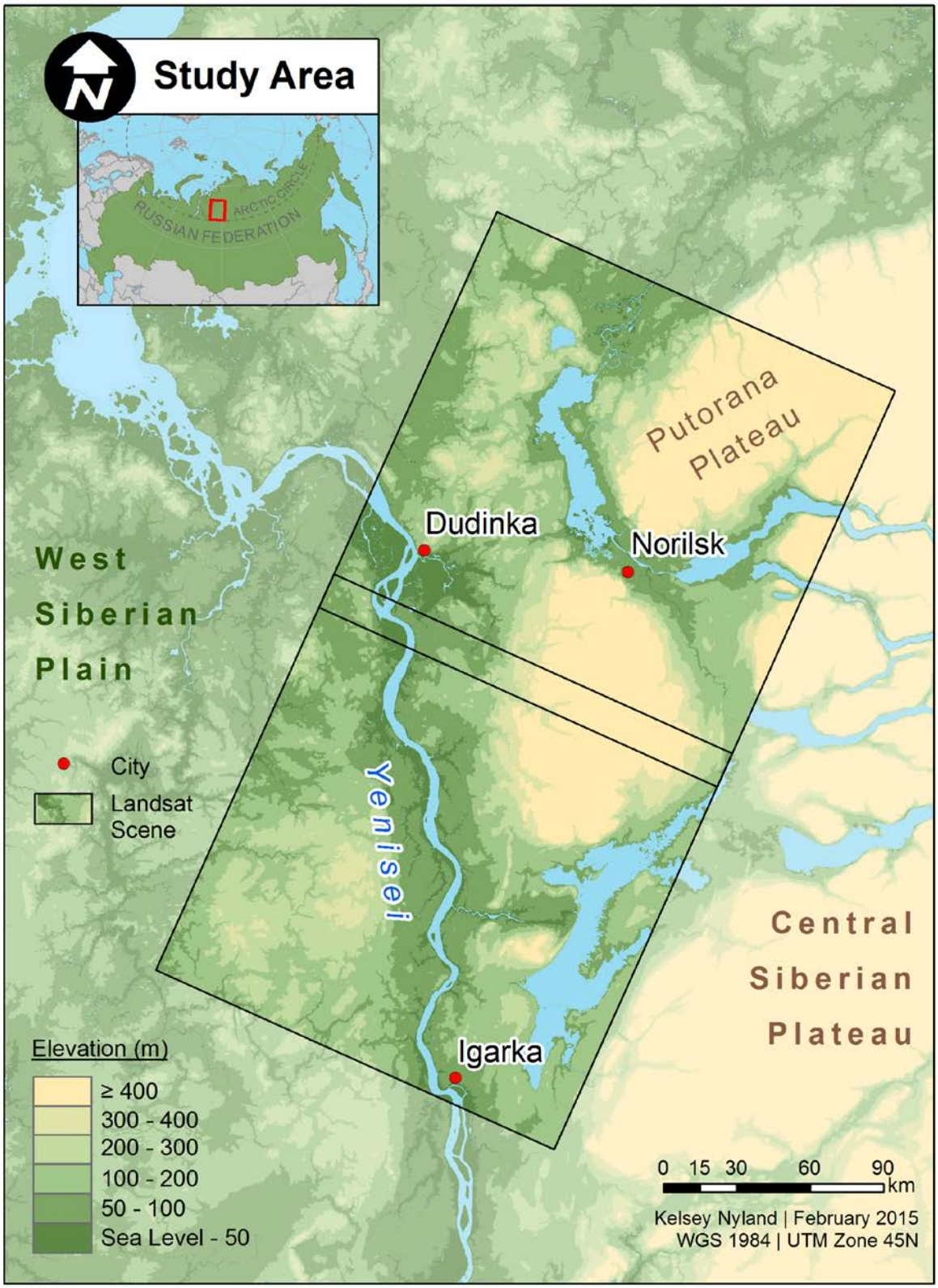

Figure 4.1. Study area map

Based on field surveying the majority of the Yenisei basin is dominated by taiga (marshy, predominantly coniferous forest) which includes species such as Siberian Larch (*Larex sibirica*), Siberian Spruce (*Pecea ovobata*), and Silver Birch (*Betula pendula*). In the lower portions of the basin, north of the Arctic Circle, tundra (marshy regions dominated by low-lying herbaceous plants and shrubs) begins to supersede the taiga landscape. Dominant plant species identified during field work in this landscape include mosses (*Sphagnum* genus), lichens (*Cetraria islandica*), grasses (*Poa* spp.), and low shrubs such as blueberries (*Vaccinium uliginosum*), dwarf birch (*Betula nana*), and alder (*Alnus fruticosa*).

Another key aspect of the lower Yenisei basin landscape is the presence of permafrost. Discontinuous permafrost underlies 10.32% of the study area, while the remainder of the area is underlain by continuous permafrost according to a digitized portion of the permafrost map of the former USSR by Yershov et al. (1991) (Figure 4.2).

Permafrost degradation has been documented through ground temperature monitoring within the discontinuous zone of the study area, in the vicinity of Igarka. Here, the depth to the active layer depth is increasing while the depth reached by seasonal freezing from the ground surface is decreasing. This means there is now a perennially unfrozen layer and that surrounding taliks are likely increasing in size. In these areas exhibiting thawing there are significant implications for increased ground water storage and the encroachment of larger plant complexes (Streletskiy et al., 2015).

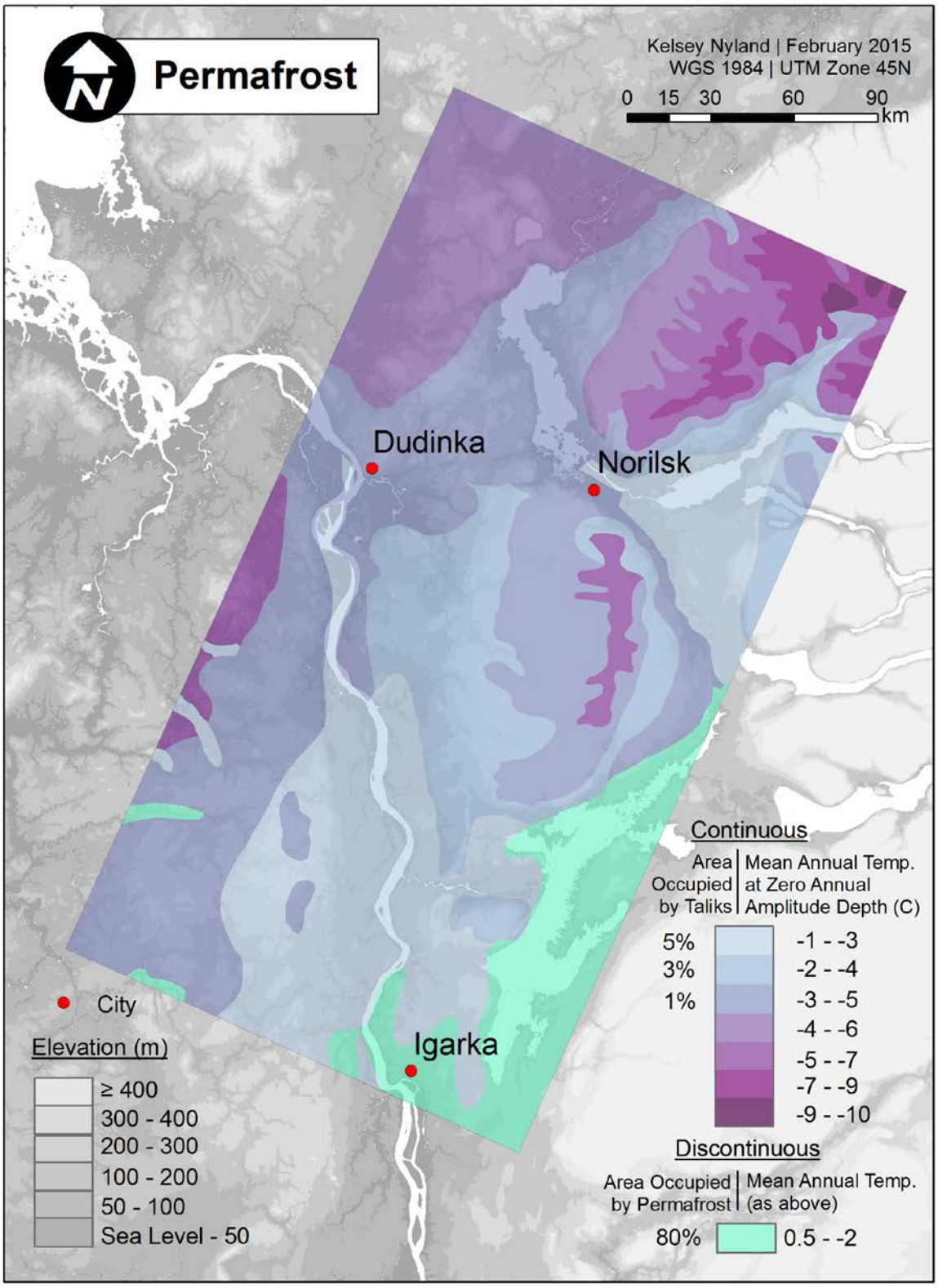

Figure 4.2. Permafrost distribution map. Digitized from Yershov et al. (1991).

There are three urban centers included within the delineated study area. The cities (from south to north) are Igarka, Norilsk, and Dudinka. The oldest of these cities is the port city of Dudinka, founded in 1667, as part of the Northern Sea Route. Both Igarka and Norilsk were founded in 1929 and 1935 respectively as GULAG labor camps for natural resource extraction and processing (Parente et al. 2012, Kozlov et al. 2009).

Igarka was once the second largest timber processer in the USSR as a deep water port with access to Dudinka and therefore the Northern Sea Route. However, the industry, which was heavily subsidized by the government during the Soviet Union, was not lucrative enough to support the city through the transition to a market economy in the 1990s. The collapse of the primary industry led to a hemorrhaging outmigration of people that continues today (Parente et al., 2012). The population of Igarka is now 28% of what it was in 1989 and continues to drop, however at a decelerated rate (Figure 4.3). Norilsk and Dudinka also experienced significant population losses of 27% and 26% respectively from 1989 to 2010, with the collapse of the Soviet Union.

Norilsk, founded for non-ferrous mining and metallurgy with its high ore content within close proximity to coal deposits (the fuel source for its smelting operations), has become the world's largest producer of nickel and palladium (greater than 20% and 40% of global production respectively), and a leading producer of platinum and copper (Groisman et al., 2012). Norilsk has also been considered the largest point source polluter throughout the global boreal region for the past 60 years (Kharuk 2000, Kozlov & Zvereva 2007, Kozlov et al. 2009, Derome & Lukina 2011, Bergen et al. 2012). Currently there are three smelting factories; Nickel Plant (est. 1942), Copper Plant (1947), and Nadezhda Plant (1979), processing the ore from the one open pit and seven

underground mines (Kozlov et al., 2009). The mining and metallurgy industry in Norilsk and the shipping business this industry brings to Dudinka's port was able to withstand the transition to a market economy with the help of private investment. This eventually affected both cities stabilizing their populations over recent years. Between 2011 and 2014, both populations have increased by 1% or by approximately 1200 people in Norilsk and 200 people in Dudinka (Rosstat 2015, Anoklin 2014).

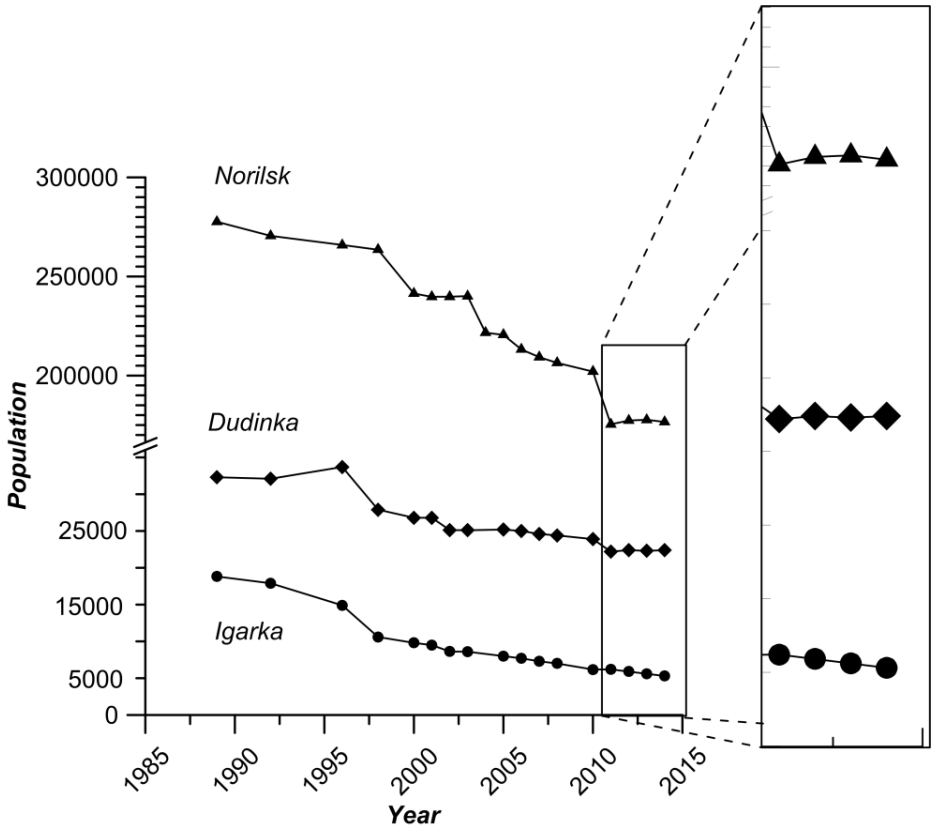

Figure 4.3. Population change in Igarka, Dudinka, and Norilsk. The magnified portion of the graph highlights the time period from 2011 to 2014, when the decreasing trend subsided for Norilsk and Dudinka, stabilizing and even slightly increasing. (Source: Rosstat, 2015)

This study area was chosen as it is the confluence of a variety of sensitive Arctic landscapes, combined with three distinct post-soviet Siberian socio-economic situations. Both the changing climatic and anthropogenic forcings are investigated through the long term land cover changes observed within the study area and in proximity to these cities through the classified time series.

Chapter 5: Methodology

5.1 Land Cover Classification Methodology

5.1.1 Data Acquisition and Preprocessing

The study area is defined by the combined scene extents of two adjoining Landsat scenes that overlap by a 50km. All of the available Landsat 5, 7, and 8 scenes for these two extents were downloaded from the United States Geological Survey's GLOVIS website archive (www.glovis.usgs.gov). The overlapping scenes are from flight path 153, rows 12 and 11 (from south to north). Scene acquisition dates ranged from the mid-1980s through August of 2014. Scenes were georeferenced as needed using second order polynomial transformations. Those scenes with 100% cloud or snow cover were removed. All Landsat 7 scenes with data gaps due to the scan line corrector failure, which occurred on March 31, 2003, were also removed from the dataset after an initial classification test was completed and residual striping was found to impact the thematic map output. The striping was caused by those stacks of images without sufficient imagery included to effectively compensate for the scan line corrector gaps. Lastly, the scenes were trimmed down to their common area as the scene extent slightly differs for each satellite. The final study area covers a total of 60,744km^2 area.

Digital Elevation Models (DEM) were downloaded from www.viewfinderpanoramas.org, a global online archive of DEMs. High latitude areas (north of 60 21'N) were not covered by the NASA Shuttle Radar Topography Mission (SRTM). Therefore, the relatively high resolution DEMs available for the Russian Arctic were created from digitized topographic maps (Ferranti & Hormann, 2012). DEMs

covering the study area were downloaded, mosaicked, and resampled using a bilinear interpolation to match the resolution, orientation, and extent of the Landsat imagery.

Initial dense time stacking classification testing also revealed that built up areas were often misclassified as water when using simple NDVI ranges or as soil when using spectral signatures through decision trees. This was due to the extremely small proportion of the scenes that are occupied by built up areas (approximately 0.1%) not allowing for it to be classified correctly without major errors elsewhere in the classified scene. In order to most accurately capture the spatial extent and changes to the urban footprints within the study area they had to be digitized. Since the built up land cover class represents such a small portion of the larger scene classifying it otherwise caused large areas to be misclassified throughout the scene. Therefore built-up areas were downloaded as open source vector data from Open Street Map (www.openstreetmap.org) and were visually assessed in comparison to scenes from each of the three time periods of interest and edited to match the extent seen in those selected images. These shapefiles were converted to a binary raster format that matched the resolution and orientation of the Landsat imagery using maximum combined area for cell assignments.

5.1.2 Land Cover Classification

All of the preprocessed Landsat images were divided into three-year time intervals. Methodological testing showed that three-year time periods allow for temporal consistency and a sufficient number of images to be included within each time stack, compensating for data gaps and cloud cover issues. The following three time intervals, 1985 – 1987 (15 images from dates spanning June 18th to September 12th), 2000 – 2002

(10 images from March 16th to October 26th), and 2012 – 2014 (11 images from April 28th to July 4th), corresponded with the two scene extents and contain a sufficient number of images within the stacks to yield a satisfactory classification. These time periods also capture key socioeconomic changes; 1985 – 1987 encapsulates the end of the Soviet era, 2000 – 2002 was near the beginning of the post-Soviet era, and 2012 – 2014 represents land use changes after 10 years of transformations resulting from the transition from a planned to a market economy.

Once the time periods of interest were established, a model was developed to classify the land covers for each period using the acquired data (Figure 5.1). For a given time stack, first, the NDVI (Equation 5.1) was calculated from the near-infrared (NIR) (Landsat 5 and 7; band 4 from 0.77 to 0.90μm, Landsat 8; band 5 from 0.85 to 0.88 μm) and red bands (Landsat 5 and 7; band 3 from 0.63 to 0.69μm, Landsat 8; band 4 from 0.64 to 0.67μm) of each image. Second, the maximum NDVI value per pixel within the stack was extracted. The resulting intermediate composite of maximum NDVI values constitutes the least cloud affected scene for the three years.

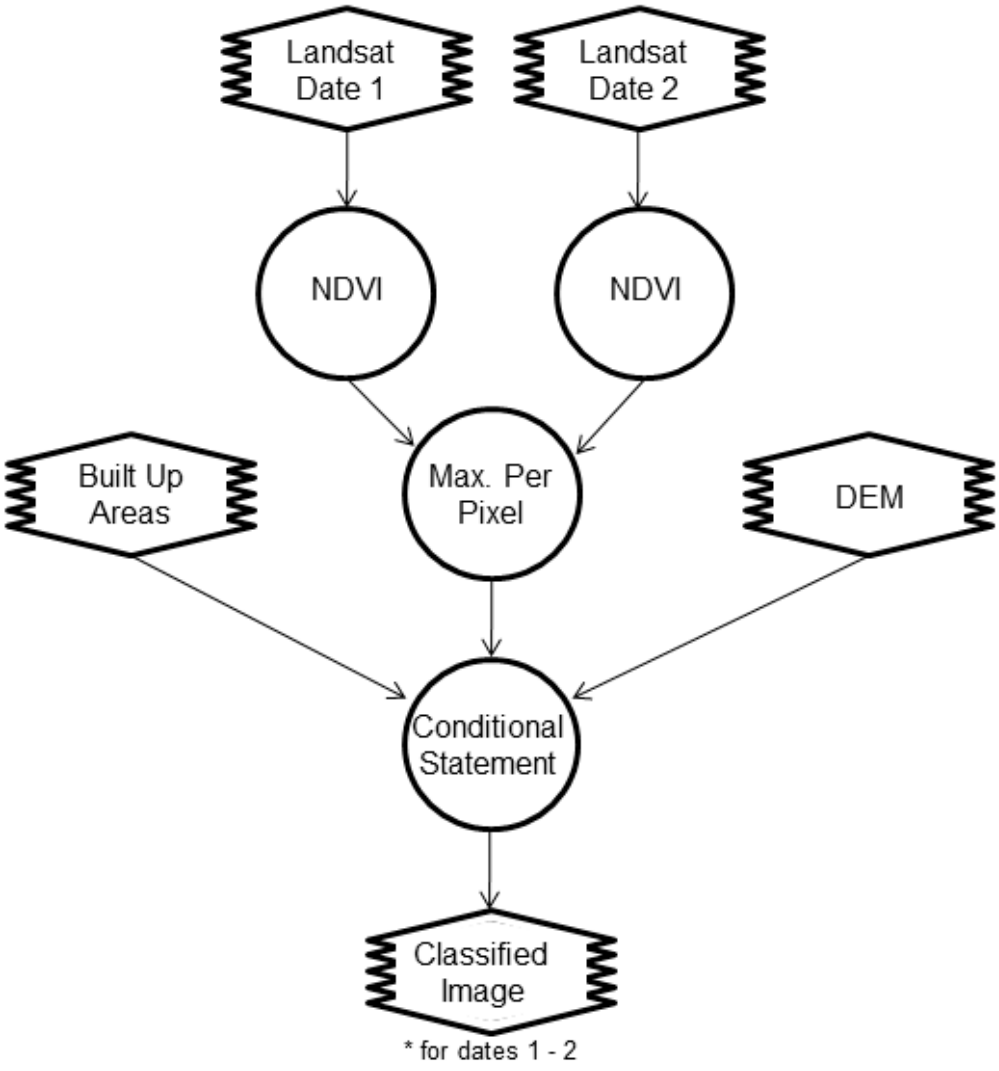

Figure 5.1. Classification model work flow diagram.

$$NDVI = \frac{NIR - Red}{NIR + Red}$$

Equation 5.1. Normalized Difference Vegetation Index (NDVI).

The data processed up to this point were linked to Google Earth and it was determined that the following five classes could be effectively classified at $30m^2$ resolution, 1) water, 2) barren ground, 3) tundra and open forest, 4) closed forest, and 5) built-up areas. These vegetative classes were previously used in an *in situ* dendrochronology study in the nearby Putorana Mountains. The determining factor in defining "open" and "closed" forests is the density of individual trees. A closed forest has abundant single tree growth and in-fill of shrubs, while an open forest has spread out tree individuals or clustered multi-stem individuals up to 10 to 20 m apart with herbaceous and moss layers in between (Kirdyanov et al., 2012). At the 30m resolution of Landsat imagery, this land cover is indistinguishable from tundra and therefore considered as one class. Thus, 15 training sites were digitized for each of the five classes in each of the time periods of interest using a combination of *in situ* knowledge from several summers of field experience with the International Permafrost Field Course, and high resolution imagery available through Google Earth, and the original Landsat scenes displayed in "true-color".

Cover Type	Classification Parameters
Water	If Max. NDVI < 0.1
Barren	If 0.1 ≤ Max. NDVI < 0.128
Tundra and Open Forest	If 0.128 ≤ Max. NDVI
Closed Forest	If 0.385 ≤ Max. NDVI and elevation < 270 m a.s.l. (Kirdyanov et al., 2011)
Built-Up	If within built-up polygons (modified from OpenStreetMap)

Table 5.1. Clauses within the classification model's conditional statement defining each of the five land cover types classified.

The maximum and minimum NDVI values for each class were then used in conjunction with local altitudinal tree line data in the third and final step in the classification model, the application of a conditional statement to the maximum NDVI, DEM, and built-up area raster to classify the entire scene (Table 5.1 and Figure 5.2).

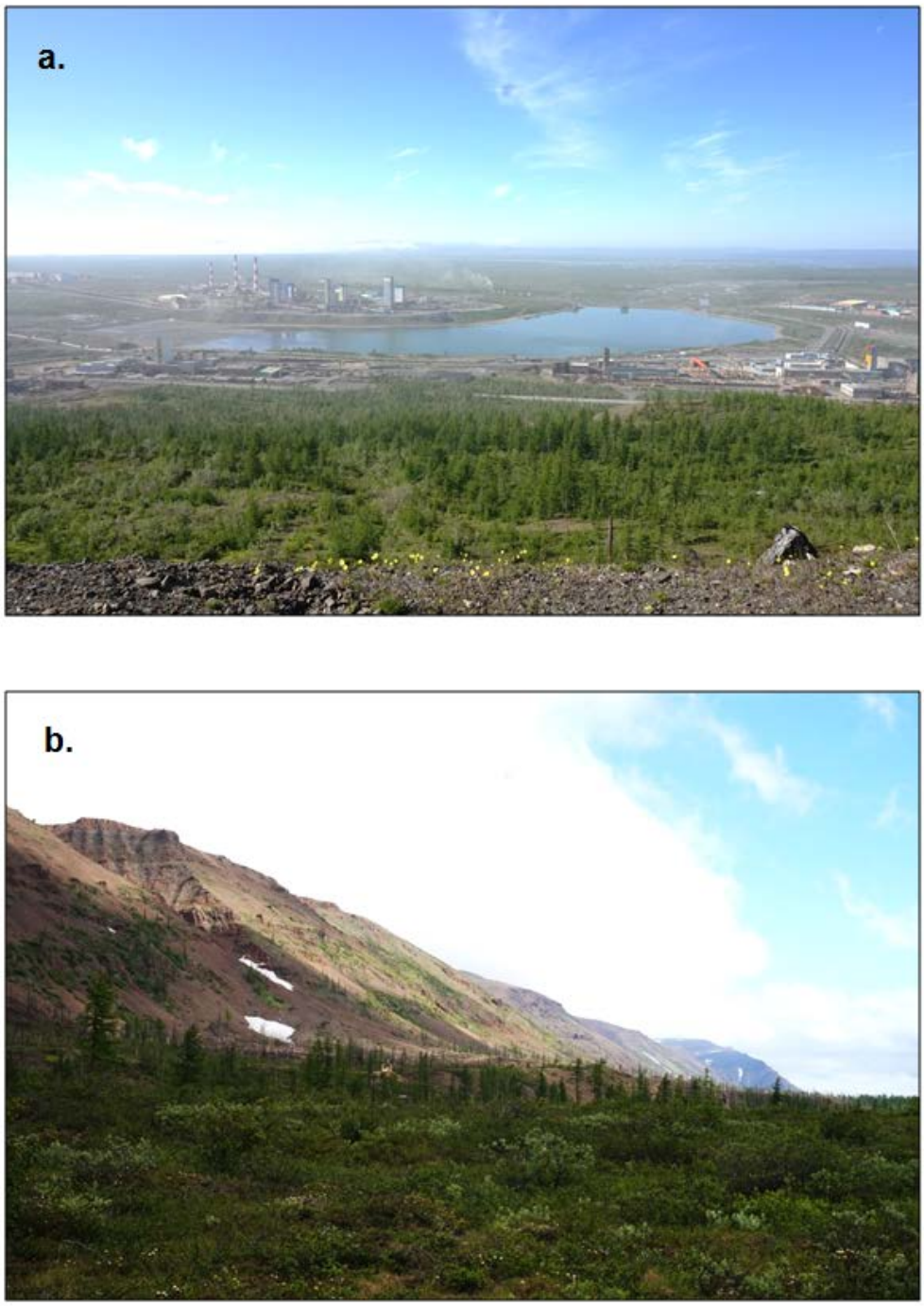

Figure 5.2. Photos of classified land covers. The background in photo a shows the built up area of Talnakh, a satellite settlement within the Greater Norilsk District, as well as an example of closed forest in the mid-ground. Photo b, taken near Talnakh, shows the steep transition up to the Plateau's barren ground and examples of an open forest in the mid-ground and tundra in the foreground (Photos by Author July, 2014).

5.1.3 Classification Accuracy Assessment Design

The thematic accuracy of a classified image is based on sampling points within the classified image, as well as a visual comparison of the final classification to higher resolution reference imagery. In an accuracy assessment of a time series spanning 29-years (1985 to 2014), the challenge resides in overcoming the amount of higher resolution imagery available, which is spatially and temporally limited. Therefore, the original Landsat images displayed in true-color were used to assess the 1985 to 1987 classified time stack, while a combination of the original scenes and higher resolution scenes from Google Earth were used for the 2000 to 2002 and 2012 to 2014 time stacks.

Numerous published equations and strategies exist for determining a representative number of samples to be collected through comparison for accuracy assessments. Many of the earlier generations of sampling recommendations were based on a binomial distribution. However, a binomial distribution is only appropriate in determining if a sampled point is simply correctly or incorrectly classified (Congalton & Green, 2008, p. 74). A more thorough understanding of error can be achieved by going beyond such a binary assessment. A multinomial distribution is required to do this, and to discover conflicting classes and other problems with the classification. Therefore the following equation (5.2), based on a multinomial distribution first proposed by Tortora (1978), was used (Congalton & Green, 2008, p. 74).

$$n = \frac{\mathrm{B}}{4b^2}$$

Equation 5.2. Multinomial equation for determining sample size.

Where *n* is the total number of samples that should be generated, B is calculated from a *chi*-square test for one degree of freedom and 1-α/*k* (where α is the significance level and *k* is the number of classes), and *b* is the absolute precision for the entire scene (Congalton & Green, 2008). A precision of 0.05 was used for this assessment, yielding a total of 663 sample points to be taken to represent the five classes.

Sample point locations were produced and visually assessed in Imagine software using a stratified random sample. This sampling scheme was chosen because it constitutes an unbiased sample selection and ensures an equal minimum number of samples in each class (Congalton & Green 2008, Plourde & Congalton 2003). Each class was assigned a minimum of 130 points. This also satisfies the rule of thumb suggested by Congalton & Green (2008) that, for areas in excess of 1 million acres, at least 75 to 100 sample points per class should be allocated. The 60,744km^2 study area is approximately equal to 15,010,170 acres (Congalton & Green, 2008).

After the stratified random sampling of 650 points per classified image were visually assessed and labeled, an accuracy report was generated using both this validation data and the classified sample data. Reports for each classified time period included a confusion matrix, overall accuracy, kappa statistic, user's accuracy, and producer's accuracy. The overall accuracy is simply the sum of the total correctly classified sampled points divided by the total number of samples as a percent (Equation 5.3). The kappa coefficient accounts to some degree for inflated overall accuracy caused by chance agreement, producing a lower result than overall accuracy (Equation 5.4) (Bishop et al. 1975, Foody 2002). Lastly, the user's accuracy represents the probability that any given pixel on the classified image is incorrectly classified due to issues with the classification

algorithm and the producer's accuracy represents the probability that the validation data were incorrectly classified through visual assessment (Equations 5.5-6) (Foody 2002, Congalton & Green 2008).

$$Overall\ Accuracy\ \% = \frac{\sum_{i=1}^{k} n_{ii}}{n} \times 100$$

Equation 5.3. Overall accuracy equation.

$$\widehat{K} = \frac{n\sum_{i=1}^{k} n_{ii} - \sum_{i=1}^{k} n_{i+}n_{+i}}{n^2 - \sum_{i=1}^{k} n_{i+}n_{+i}} \times 100$$

Equation 5.4. Kappa coefficient equation.

$$User's\ Accuracy\ \% = \frac{n_{ii}}{n_{i+}} \times 100$$

Equation 5.5. User's accuracy equation.

$$Producer's\ Accuracy\ \% = \frac{n_{ii}}{n_{+i}} \times 100$$

Equation 5.6. Producer's accuracy equation.

Where *n* is the number of samples for class *i*, and *k* is the total number of classes. The user's and producer's accuracy equations shown above are essentially marginal calculations for each row and column of the generated accuracy matrix respectively (Foody, 2002).

5.2 Quantifying Land Cover Changes

Maps using the total relative changes calculated for each of the classified land cover classes were created to illustrate the spatial extent in both the expansion and reduction in land covers. One important note is that to observe the true static changes in surface hydrology all rivers and small seasonal ponds (< 40 ha) were removed from the change detection maps as they are subject to seasonal fluctuations which can be impacted by the distribution of scenes within a time period (Smith et al., 2005).

5.3 Spatial Climate Data Acquisition and Preprocessing

There are multiple archived climate datasets that provide an enhanced spatial dimension to climate change analyses besides traditional observation networks (e.g. Serreze & Hurst, 2000). Of these the NASA Modern Era-Retrospective Analysis for Research Applications (MERRA) project has been found to one of a few reanalysis products that displays minimal bias and is more consistent with independent Arctic observation data for the nearly 30-year time period investigated in this study (Lindsay et al., 2014).

Spatially based climate data for the study area extent was acquired from the NASA Modern Era-Retrospective Analysis for Research Applications (MERRA) project produced by the Global Modeling and Assimilation Office. Reanalysis products such as this hybridize satellite observations with modeled fields to retroactively recreate spatially consistent climate data. The data is based on climatologic reanalysis of the satellite era (1979 to present) using the Goddard Earth Observing System version 5 (GEOS-5) atmospheric general circulation model to assimilate observation data from six hour

intervals over a 2/3° longitude by 1/2° latitude global grid (Bosilovich 2008, Reinecker et al. 2011).

Monthly mean temperatures were obtained for the coarse resolution MERRA climate data covering the Landsat time series used for classification (June 1985 to August 2014). An additional year was included at the beginning of the time series to create a 30-year climate normal (August 1984 to August 2014) for analysis. The spatial extent of the data was equal to the processing extent of the study area yielding an 11x7 grid. Within the grid 50 pixels are included within the study area. The monthly data were then aggregated to 5-year mean to examine the spatial and temporal trends of air temperature at 2m height, precipitation, and snow.

Chapter 6: Results and Discussion

6.1 Land Cover Classification

The classification model described in the previous section produced the following three thematic maps from the stacked two year time periods. Together they span a total of 29 years from 1985 to 2014 (Figure 6.1). The subsequent accuracy assessments revealed that the overall accuracies are, in chronological order, 85.86%, 88.77%, and 87.23%. The increasing accuracy of the maps over time is more likely a result of the increased area covered by higher resolution imagery on Google Earth and therefore easier and more accurate visual assessment of validation points used in the accuracy assessments.

While, these results prove acceptable for evaluating the land cover changes that have taken place, it is important to note where the deficiencies lie in this classification. Note the confusion matrices for each map shown in tables 6.1 a-c. They illustrate that the three consistently confused classes throughout the map series are tundra and open forest being misclassified as barren or closed forest, and closed forests misclassified as tundra and open forests. The distinction between tundra / open forest and closed forests is difficult to visually identify and difficult to classify when assigning validation points, particularly where these two classes are highly heterogeneous, such as in the center of the study area. This is also true for the distinction between tundra / open forest and barren ground at high elevations, such as on the plateaus included in the northeast quadrant of the study area. However, the producer's accuracies for these classes are consistently lower that than the user's accuracies, indicating that the instances of misclassified pixels

are more likely due to the classification parameters. However, lack of extensive higher resolution imagery available for the generation of validation data for validation purposes may be the bigger cause of calculated error. The extent of high resolution imagery available for the study area on Google Earth increases significantly after the mid-2000s. More high resolution imagery improves the ability to visually identify that land cover for generating validation data.

Despite all of these issues, the three classifications accuracies when also accounting for chance agreement between validation and classified samples, or the kappa statistic, are (again in chronological order), 0.8231 (82.31%), 0.8596 (85.96%), and 0.8404 (84.04%). As all of these values are greater than 0.8, it indicates strong agreement between the three classifications and their individually generated validation data (Landis & Koch, 1977). Therefore these maps are satisfactory for further spatial analysis of the region.

The proportions of area occupied by the land covers in each map were calculated (Figure 6.2). A chronological comparison of these proportions shows a generalized 'greening' trend, or the expansion in the total area occupied by the dense shrubs and trees that make up closed forests, as well as a reduction in tundra / open forests and barren ground. Over the entire 29 years, the closed forests expanded by roughly 10% of the total area (approximately 414km^2), along with a 9% (approximately 372km^2) reduction in tundra and open forests and a 2% (approximately 83km^2) decrease in barren ground. This trend is confirmed by numerous studies performed for the circum-Arctic and Central Siberian region that looked at the northward encroachment and altitudinal climbing of shrubs previously discussed (e.g. Macias-Fauria et al. 2012, Kirdyanov et al. 2012, Tape

et al. 2006). In addition, there is a slight (1%, or approximately 41km^2) increase in the area occupied by lakes. The changes observed for each of the classified land cover types will be discussed in detail in the following sections.

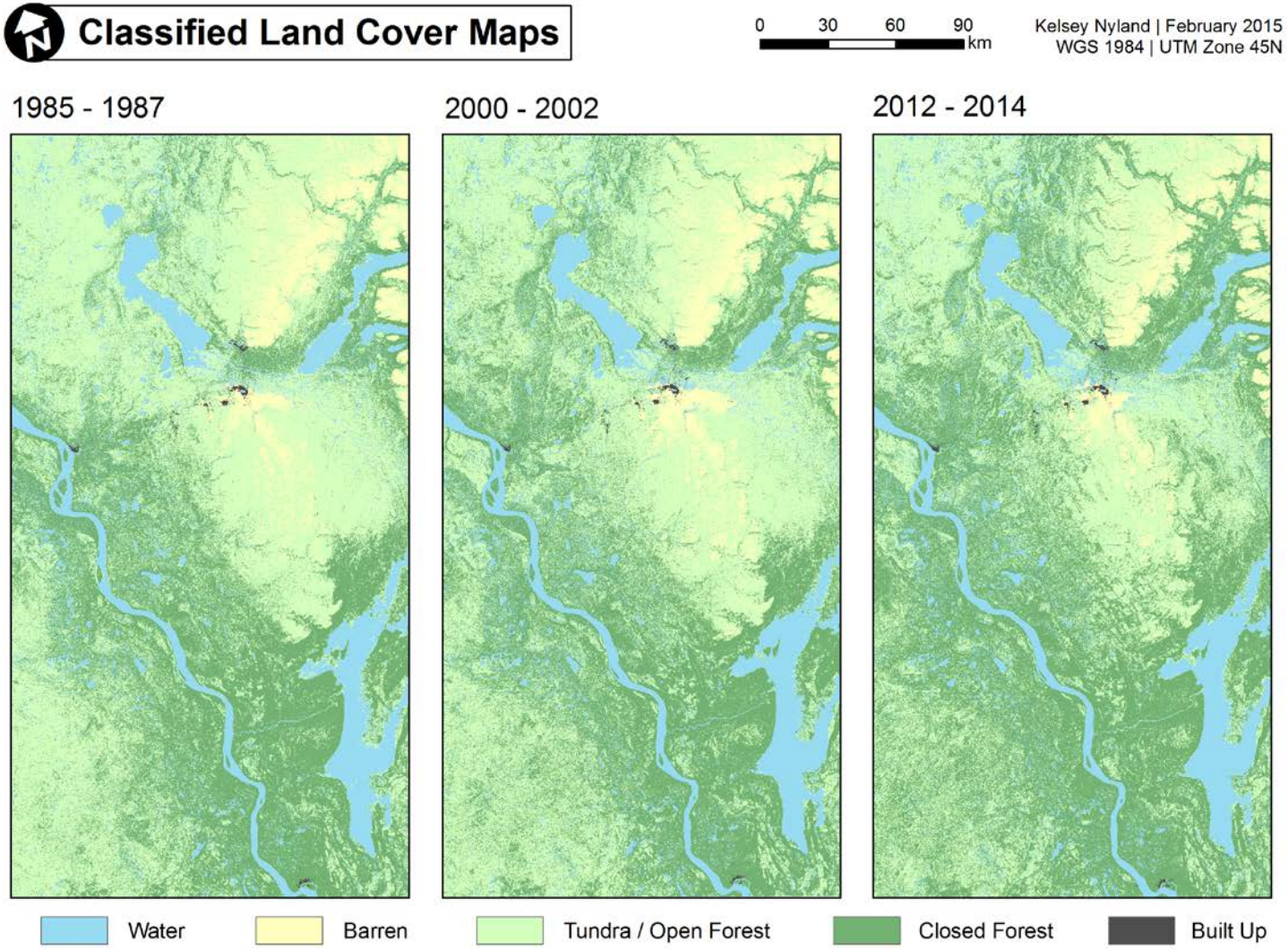

Figure 6.1. Thematic maps of land cover in the Lower Yenisei for three time periods. Results of classification of Landsat dense time stacking.

a.

1985 - 1987	Verification Data (Known Cover Types)					
Classification Data	Water	Barren	Tundra / OF	CF	Built Up	User's Accuracy
Water	122	3	4	1	0	93.85%
Barren	15	84	30	0	1	64.62%
Tundra / OF	2	1	118	9	0	90.77%
CF	0	0	12	118	0	90.77%
Built Up	0	2	8	4	116	89.23%
Producer's Accuracy	87.77%	93.33%	68.60%	89.39%	99.15%	

Overall Accuracy = 85.86% **Kappa Statistic = 82.31%**

b.

2000 - 2002	Verification Data (Known Cover Types)					
Classification Data	Water	Barren	Tundra / OF	CF	Built Up	User's Accuracy
Water	125	1	4	0	0	96.15%
Barren	5	98	25	0	2	75.38%
Tundra / OF	1	4	115	10	0	88.46%
CF	0	0	6	124	0	95.38%
Built Up	1	5	6	3	115	88.46%
Producer's Accuracy	94.70%	90.74%	73.72%	90.51%	98.29%	

Overall Accuracy = 88.77% **Kappa Statistic = 85.96%**

c.

2012 - 2014	Verification Data (Known Cover Types)					
Classification Data	Water	Barren	Tundra / OF	CF	Built Up	User's Accuracy
Water	121	2	5	2	0	93.08%
Barren	7	106	16	1	0	81.54%
Tundra / OF	3	1	111	15	0	85.38%
CF	4	0	12	114	0	87.69%
Built Up	2	5	7	1	115	88.46%
Producer's Accuracy	88.32%	92.98%	73.51%	85.71%	100%	

Overall Accuracy = 87.23% **Kappa Statistic = 84.04%**

Table 6.1. Confusion Matrices for the a) 1985-1987, b) 2000-2002, and c) 2012-2014 classified thematic maps. Also included are the kappa, overall, user's, and producer's accuracy statistics.

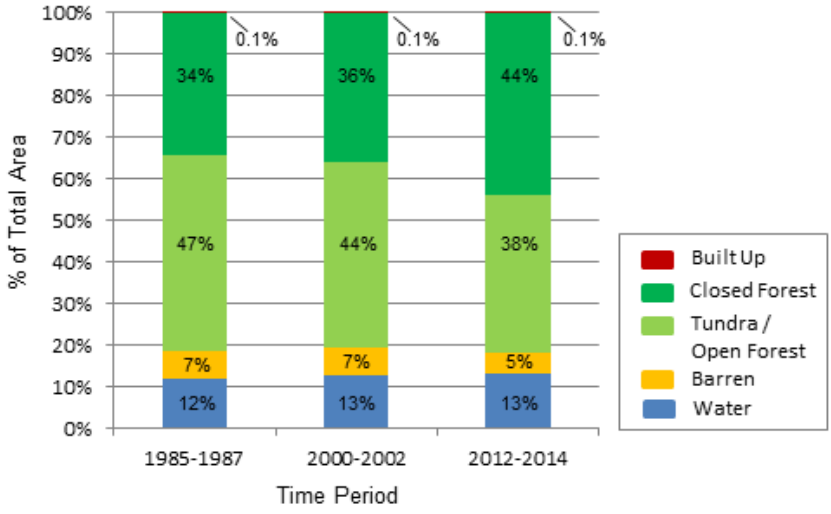

Figure 6.2. Land cover proportions for each classified time stack.

6.2 Regional Climate Change in the Lower Yenisei

6.2.1 Spatial Climate Reanalysis

30-years of NASA MERRA data produced the following maps, illustrating five year means (the first two rows of maps) of air temperature at 2m height, precipitation, and snow, as well as the difference between the first and last averages (lower left map) and the rate of annual change per pixel (the eighth map in the panel) (Figures 6.3-5). These spatial climate patterns, concurrent with the classified time series, might be reflections of general trends observed for the greater western Eurasian region (Overland et al. 2014, Derksen et al. 2014). They provide some explanation for the observed land cover changes to be discussed in the following sections.

Air temperatures at 2m height display a marked general increase throughout the region for the 30-year time period. Within the delineated study area, the average

temperature increased at an average rate of 0.05°C/year yeilding a 1.22°C average warming across the scene. While the increase is marked throughout the region, it is more pronounced in the northern portions of the scene, as depicted in the lowland area north of the Putorana Plateau. This is also where the temperatures are increasing at the fastest rates (Figure 6.3).

Total annual precipitation within the study area has decreased at a rate of -4.49mm/year to an average of 16.45mm. However, this spatially averaged trend is not true of the entire area. While the northern portions of the scene have experienced conspicuous decreases, the southernmost portion displays a consistant increase in total annual precipitation (Figure 6.4). Snow, while part of the total precipitation, displays slightly different spatial trends. The maximum annual snow depth within the study area decreased on average by 0.104m at a rate of -0.005m/year. Across the region as a whole, decreasing snow is primarily occuring in the northwest, cutting diagionally through to the southeast. Contrary to this trend are areas of high elevation that display slightly deeper maximum snow depths, though the trend across the scene is negative (Figure 6.5).

Increasing air temperatures have caused ground and therefore permafrost warming and in some areas degredation (e.g. Romanovsky et al. 2010, Fedorov et al. 2014). These results show that the Lower Yenisei is no exception to this larger trend.

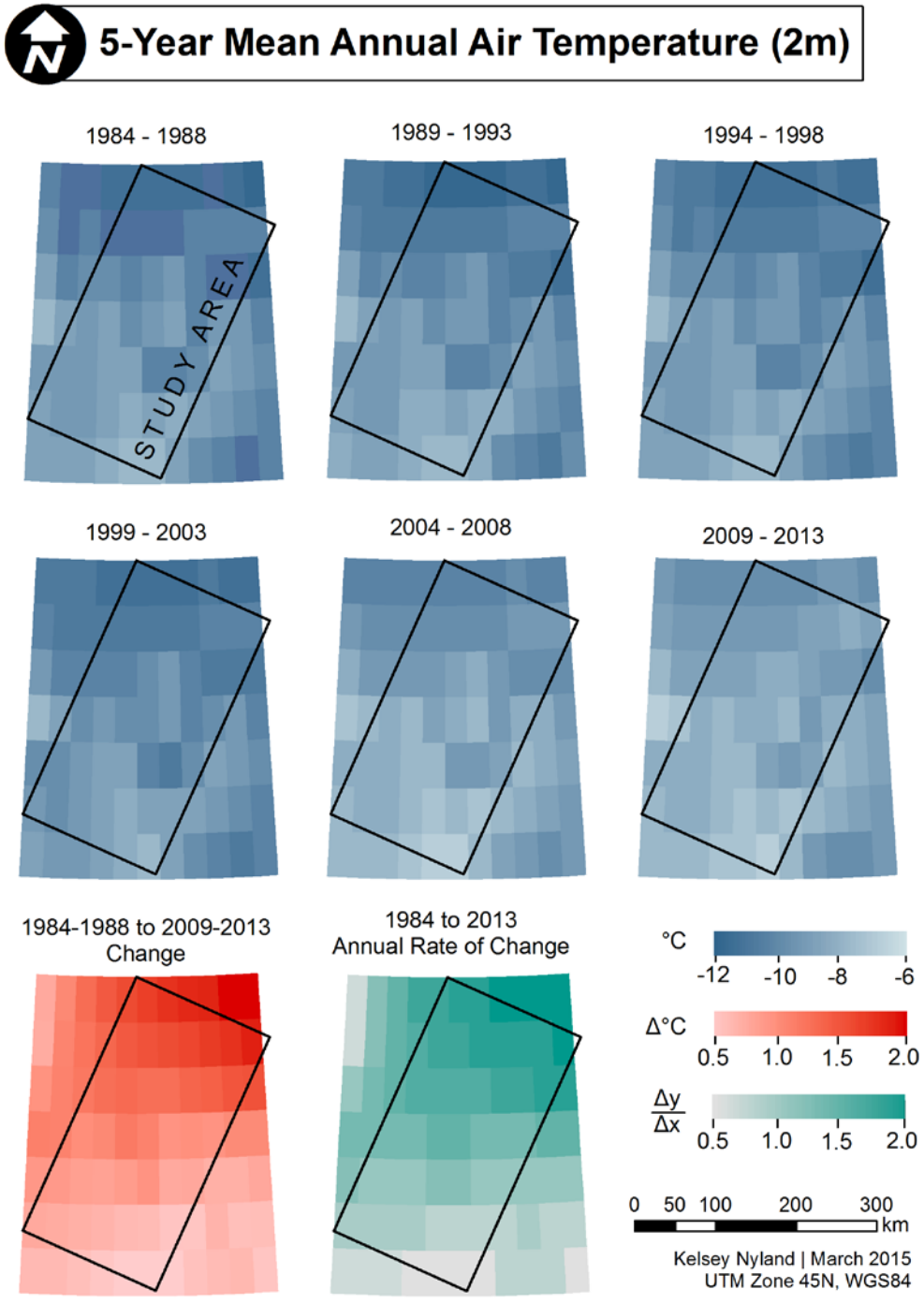

Figure 6.3. Panel graphic displaying six five-year means of mean annual air temperature (C°), the difference in temperature from 1984 to 2013, and the rate of change for the 30-year time period. Data source: NASA-MERRA.

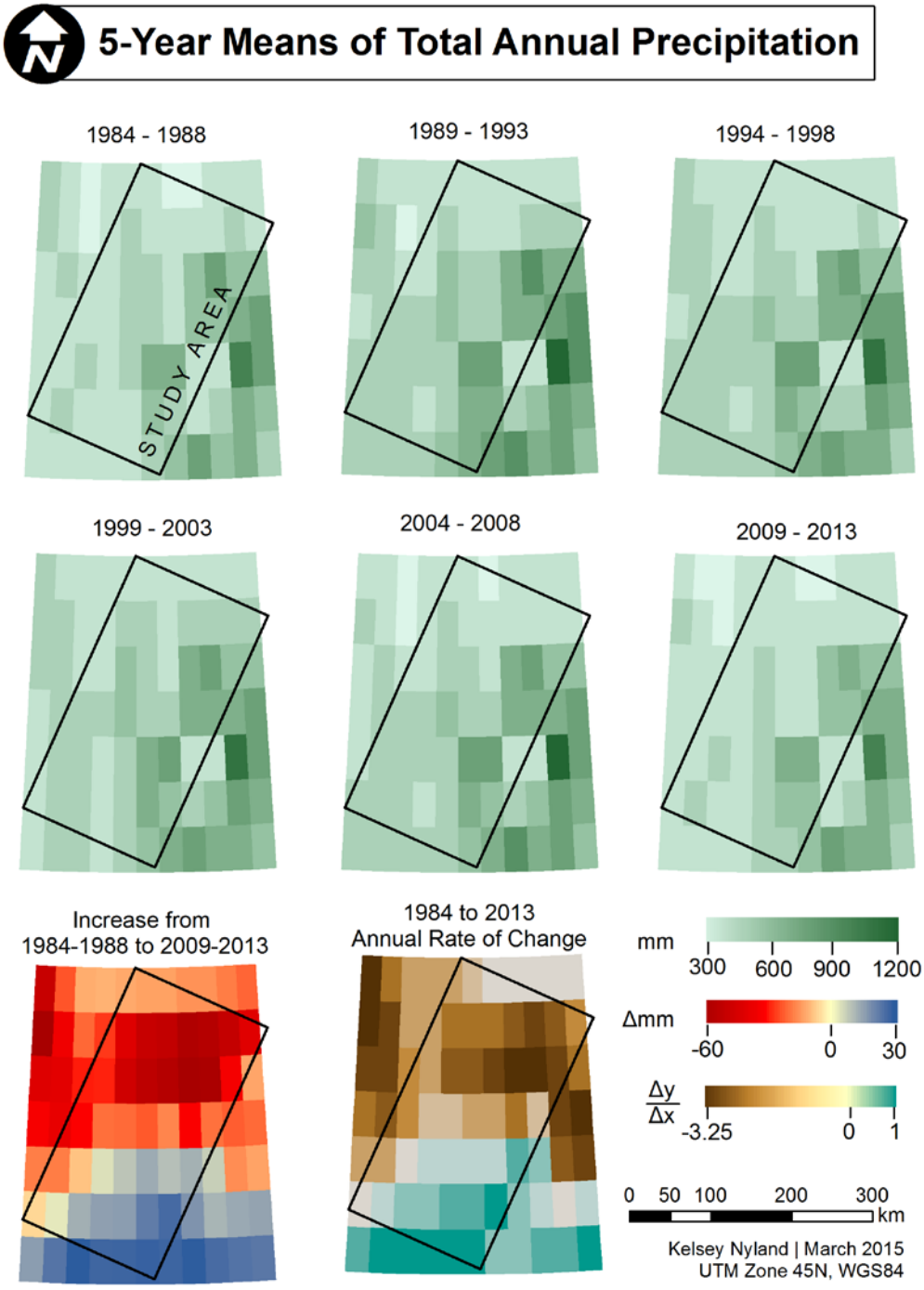

Figure 6.4. Panel graphic displaying six five-year means of total annual precipitation (mm), the difference in temperature from 1984 to 2013, and the rate of change for the 30-year time period. Data source: NASA-MERRA.

Figure 6.5. Panel graphic displaying six five-year means of maximum annual snow depth (m), the difference in maximum depth from 1984 to 2013, and the rate of change for the 30-year time period. Data source: NASA-MERRA.

6.2.2 Weather Station Climate Analysis

To validate the spatial reanalysis climate data, observational data from within the study area were also examined. Data from the World Metorological Organization (WMO) was obtained from weather stations located near the cities of Igarka and Norilsk, representative of the southern and northern portions of the study are respectively, for the same time period (1984 – 2014) as the NASA MERRA data (Figure 6.6).

Confirming the results from the reanalysis data, both stations recorded significant increases in air temperatures. Mean annual air temperature have increased at an average rate of 0.05˚C/year in Igarka and by 0.045˚C/year in Norilsk. Also, the total annual precipitation in Igarka has been increasing at an average rate of 2.4mm/year. However, contrary to the reanalysis data, the total annual precipitation at the Norilsk station has also been increasing at an average rate of 2.7mm/year.

The conflicting precipitation results between the reanalysis generated data and the point location observations can likely be attributed to discrepancies due to spatial aggregation and local variability. The permafrost-precipitation-atmosphere interaction is complex and remains poorly understood, though it is clear that it is highly dependent on the local redistribution of snow. The coarse nature of the NASA-MERRA data, while providing insight into spatial regional-scale climatic trends, does not provide sufficient information on the local accumulation and redistribution of snow, which tends to occur in valleys and depressions. The highly localized variations in snow accumulation exert significant impacts on local vegetative covers, as well as ground temperature.

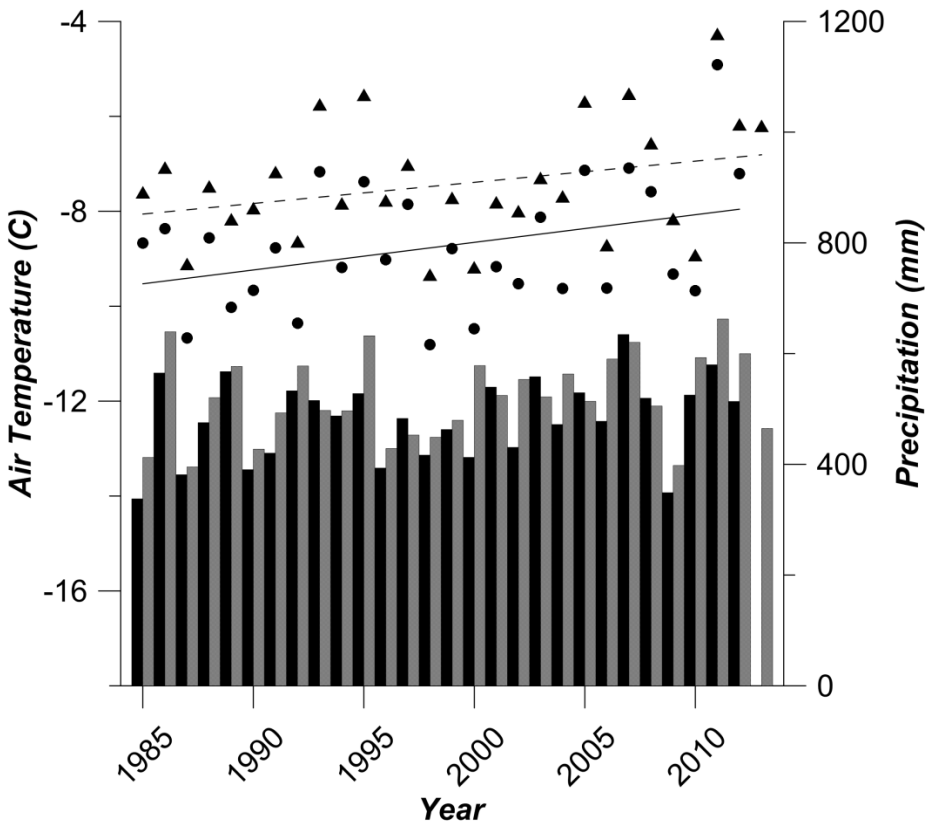

Figure 6.6. Climate data from weather stations near the cities of Igarka and Norilsk. Where data from Igarka is represented by triangles, the dashed trend line for mean annual air temperatures, and the grey bars for precipitation, and data from Norilsk by the circles, solid line, and black bars. Data source: WMO.

6.3 Regional Climate Induced Land Cover Change

6.3.1 Surface Hydrology Change

The nature of the dense time stacking methodology, utilizing all available imagery in the attempt to create a "best representation" composite image, can be problematic for evaluating long-term surface hydrology changes. The aerial extent of rivers and small lakes can be highly variable depending on the date of image acquisition. For example, if

a given time stack has the majority of its images from spring or early summer it may artificially inflate the total area occupied by water by capturing seasonal inundation from snow melt (Karlsson et al., 2012, 2014). In order to capture only the long-term changes to thermokarst lakes, findings from previous works that also used Landsat imagery were used to develop perquisite conditions to limit waterbodies observed for static changes. First, all rivers, streams, and lakes smaller than 40ha were removed, as they are either highly sensitive to seasonality or are ephemeral in nature (Smith et al., 2005). Second, “no-closure” lakes (those connected to river systems through tributaries) were also removed, as connections to river systems also make these more variable than closed lakes on an intra-annual basis (Chen et al., 2013).

The resulting difference maps show areas of long-term lake expansion and contraction over the first and second half of the time series, and for the entirety of the observed 29 years (Figure 6.7). All subsequent land cover class changes to be discussed will also be displayed in this fashion. It should be noted that the percentage of change displayed on the map is exaggerated due to "raster pyramids" built for display purposes which down-samples the resolution for faster display and printing purposes.

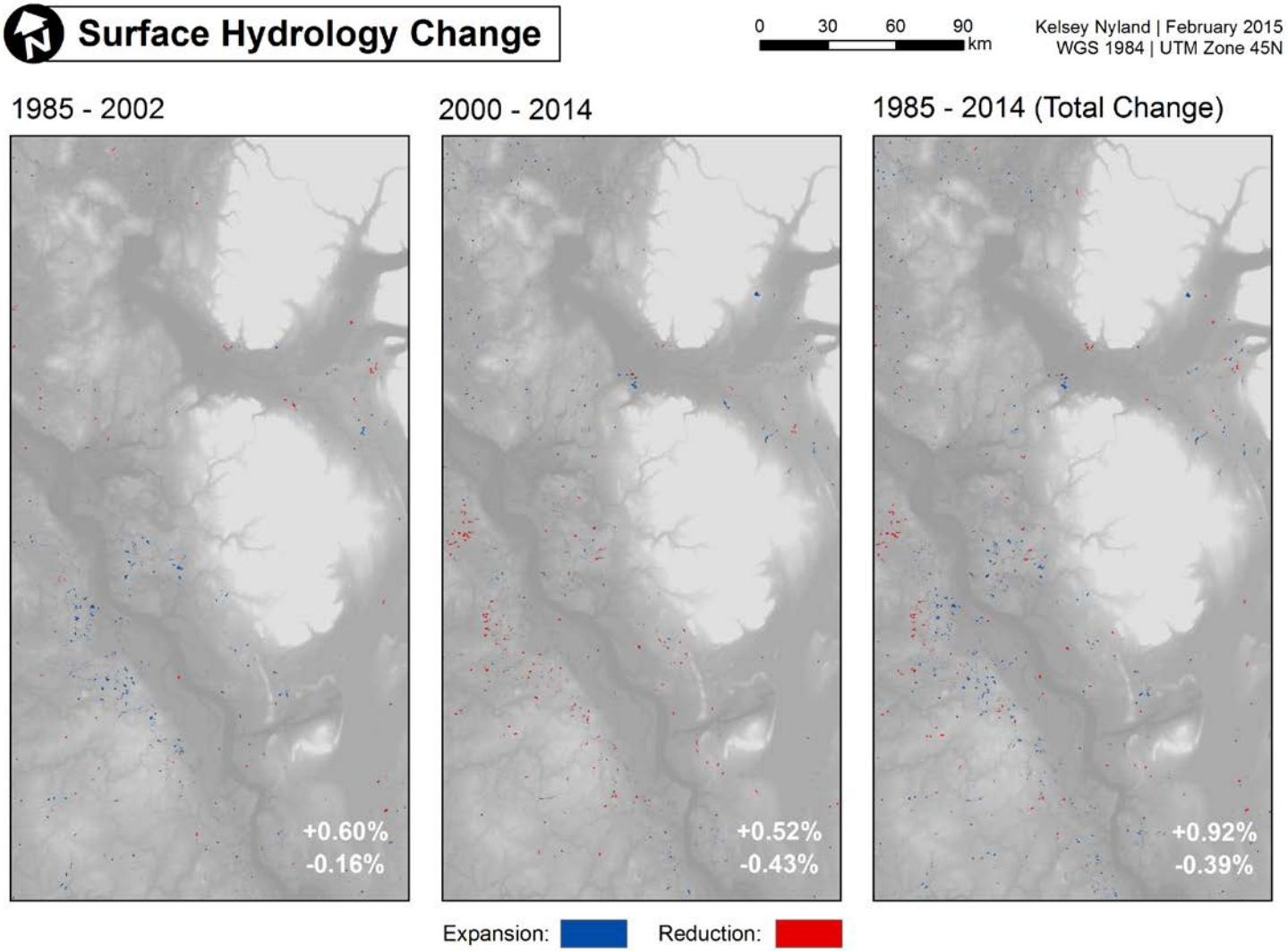

Figure 6.7. Difference maps showing the expansion and reduction for large lakes (>40ha) and the percent change in the Lower Yenisei for the classified time period.

Over the course of the time series, the total lake area and total number of observed lakes has increased by 11.23% and 15.99% respectively, and the majority of these increases occurred during the first half of the time period from the mid-1980s to the early 2000s (Figure 6.8). This indicates permafrost thaw and therefore degradation (e.g. Yoshikawa & Hinzman 2003, Smith et al. 2005, 2007, Karlsson et al. 2014). Throughout the study area, while the vast majority of the thaw lakes have expanded, and in some instances new lakes have appeared, there are also a number of lakes that either shrank or disappeared (Figure 6.9). While a minority of these changes could be attributed to the increases in air temperature and decreased precipitation found in the analysis of the NASA-MERRA data, it has also been interpreted as an indication of discontinuous permafrost degradation (e.g. Smith et al. 2005, Yoshikawa & Hinzman 2003, Karlsson et al. 2014). This also supports the general trend of increasing lake area and number of lakes as it overcomes any additional evaporative processes occurring.

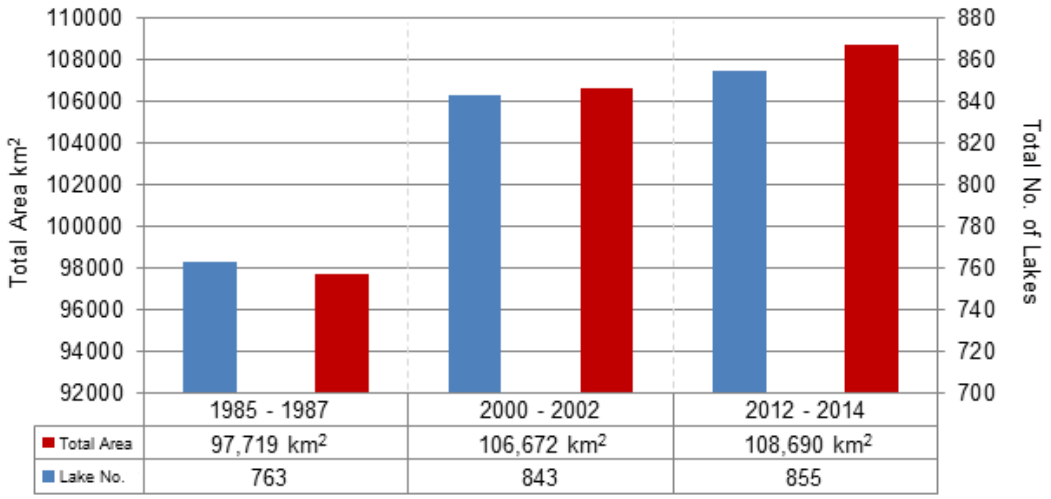

Figure 6.8. Changes in total large lake (>40ha) area and total number of large lakes in each classified time period. Note the greatest increase occurred during the 13 years between 1987 and 2000.

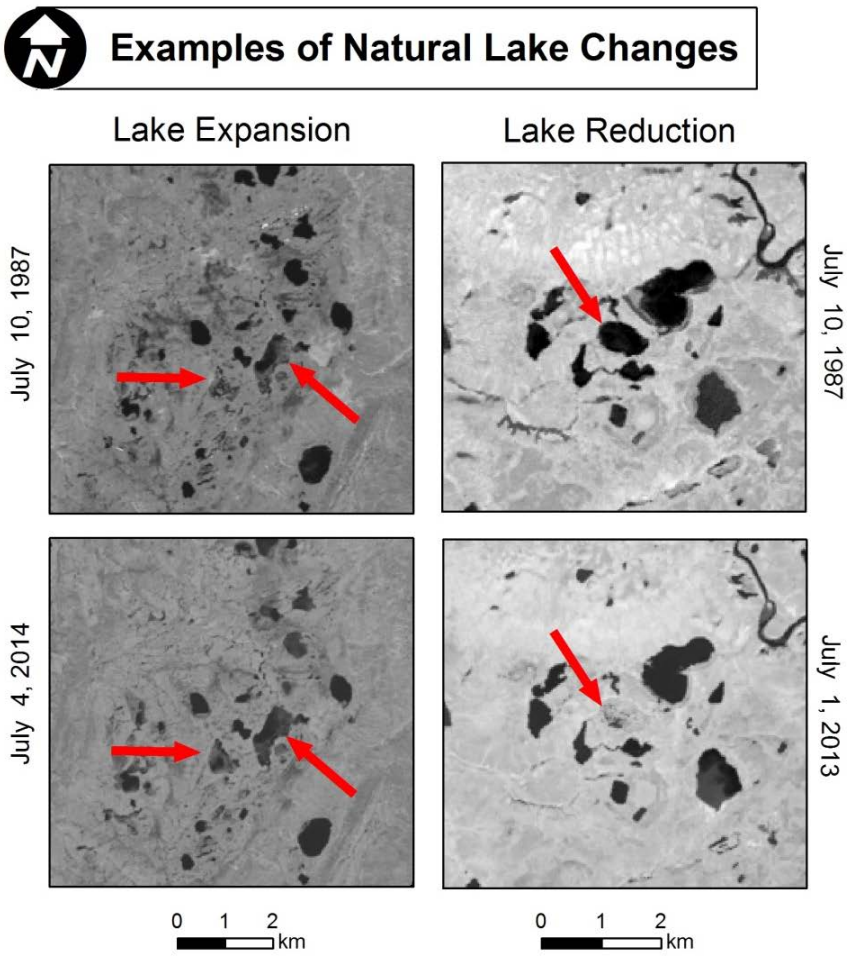

Figure 6.9. Examples of lake changes in areas not directly affected by anthropogenic activities taken from original Landsat scenes displayed in grey scale. The two left hand images show lake expansion and appearance in tundra and open forest and the two right hand images show a lake drain in an area of mixed closed and open forest where there is likely a talik.

6.3.2 Vegetative Change

The three land cover classes, barren ground, tundra and open forest, and closed forest are closely linked through their spatial patterns of change. Three distinct spatial vegetative trends were identified within the classified time series; 1) tundra and open forest densification and therefore transition to closed forest, 2) a rising treeline or the transition from barren ground to tundra / open forest or closed forest at elevation, and 3) pollution caused vegetation damage and removal followed by subsequent reclamation, or the transition back to tundra / open forest or closed forest. Each of these trends can be observed in the classified time series and can be confirmed by independent *in situ* studies. The third identified trend however, evident in the area to the southeast of the Norilsk industrial complex, will be examined closer and discussed in section 6.5 as it is an anthropogenic-induced change.

The first two identified trends (the densification of tundra and open forests, and the rising altitudinal tree line) (Figures 6.10-12) are both validated by a recent *in situ* vegetative studies. One was a transect study conducted in the Putorana Mountains to the northeast of the study area (Kirdyanov et al., 2012) and the other was a pan-Russian study of shrub expansion with one site located approximately 25km northeast of the city of Dudinka (Frost & Epstein, 2014). They both cite increasing snow accumulation, protecting tree and shrub growth in winter, as the likely primary driver behind the expansion of these plant communities (Kirdyanov et al. 2012, Frost & Epstein 2014). This is supported by the climate analysis conducted in this work that found that, while generally decreasing across the region, snow depths at elevation have increased.

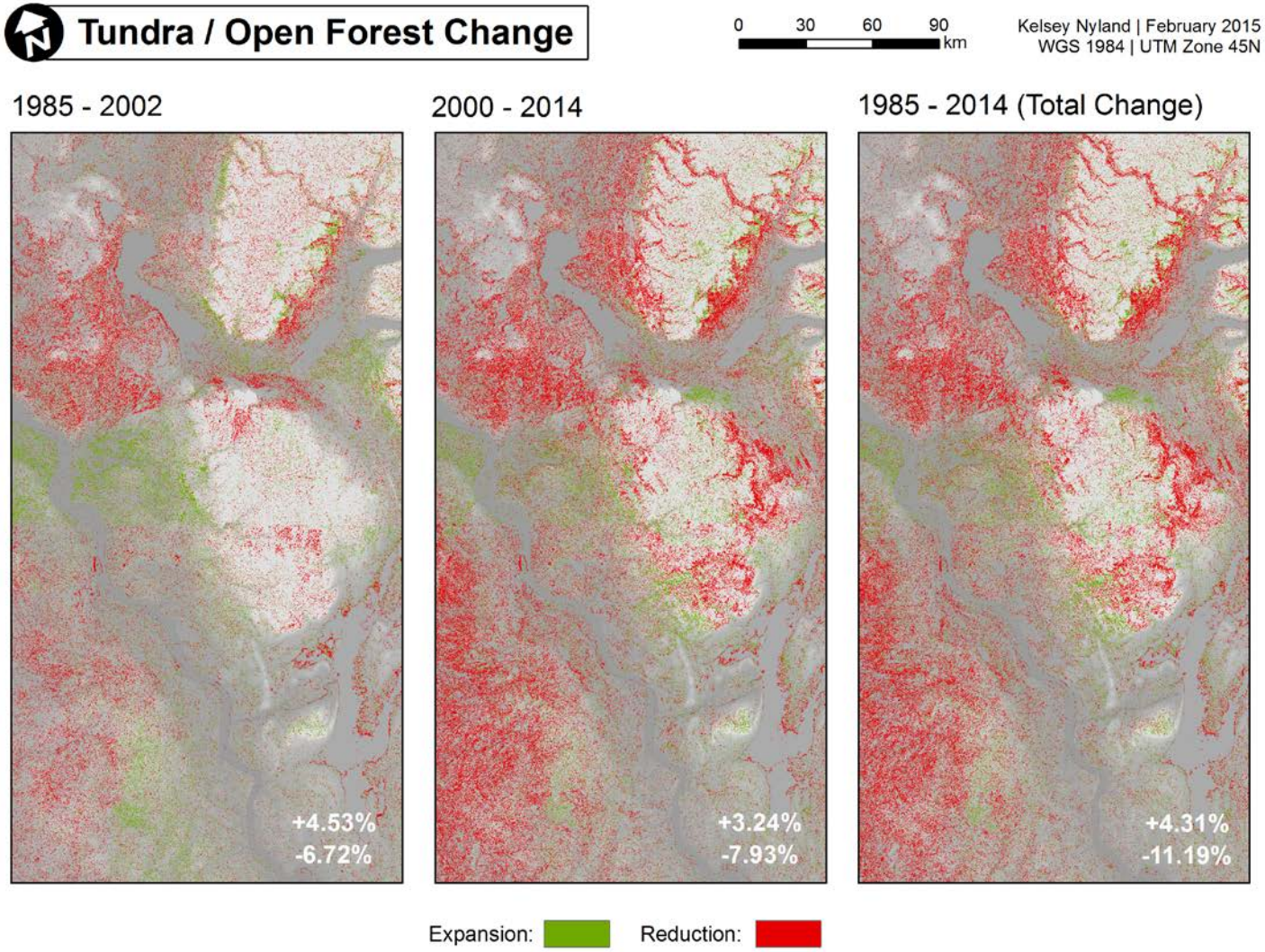

Figure 6.10. Difference maps showing the expansion and reduction in area occupied by tundra and open forest and the percent change for the classified time period.

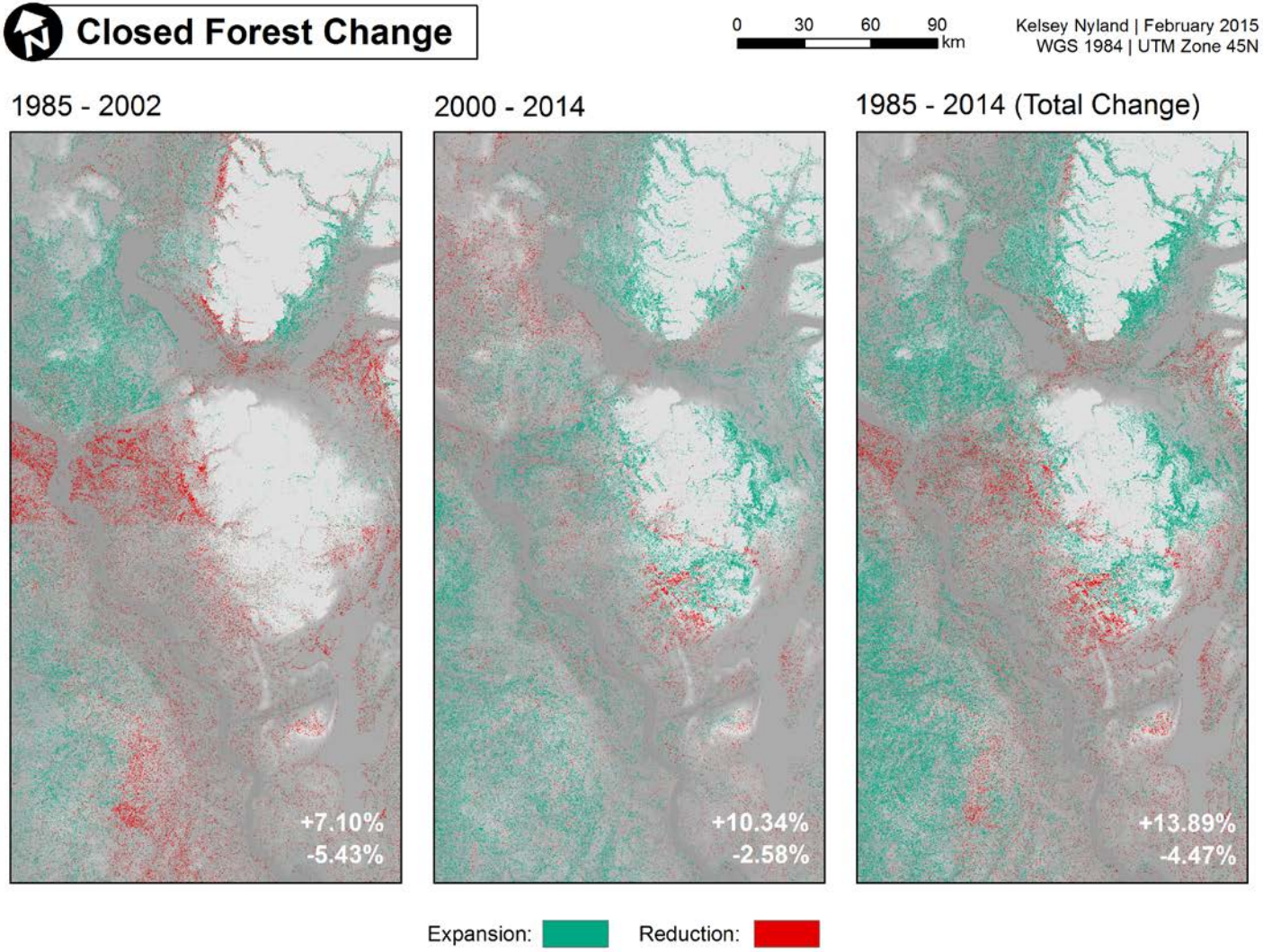

Figure 6.11. Difference maps showing the expansion and reduction in area occupied by closed forests and the percent change for the classified time period.

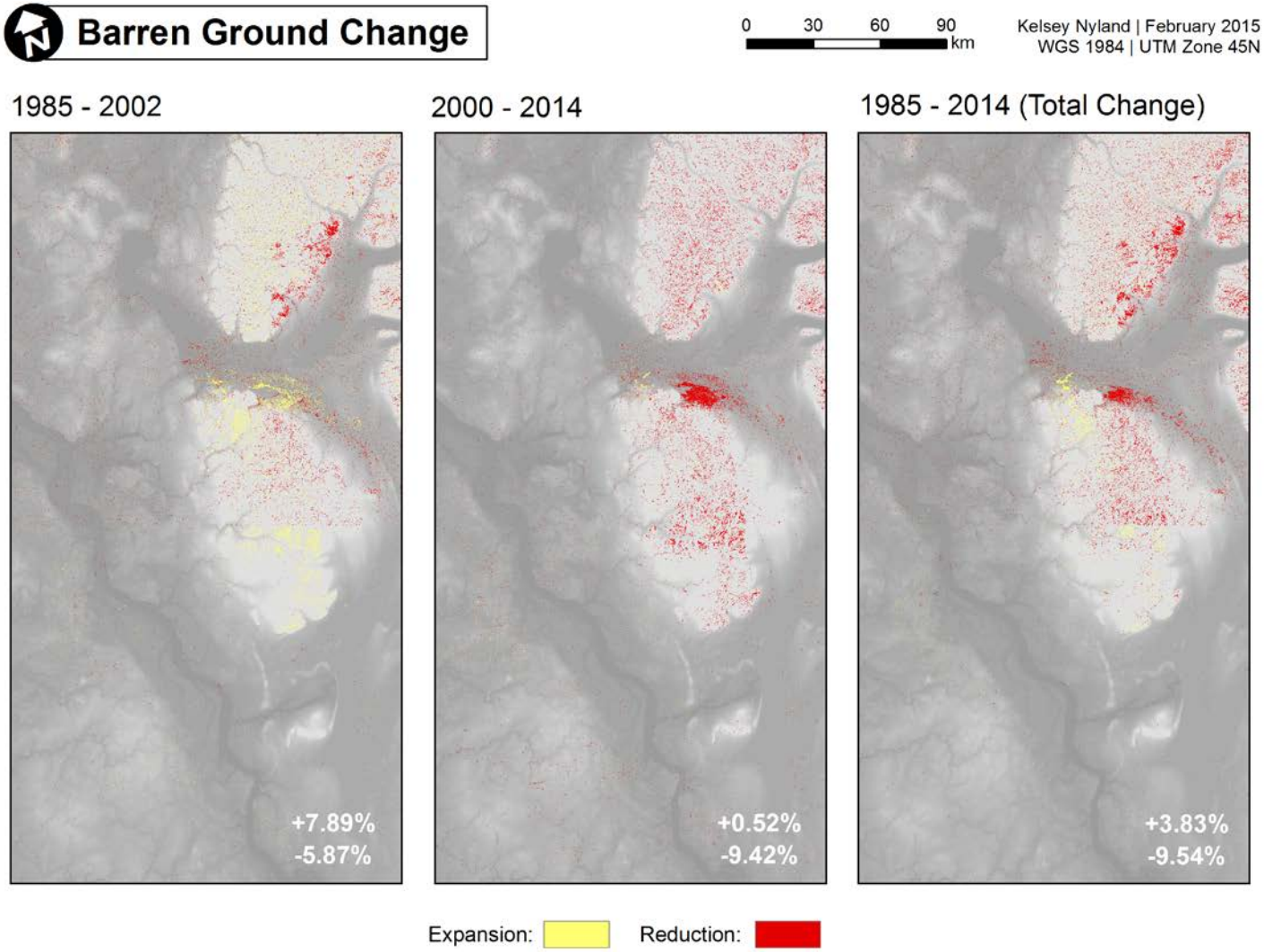

Figure 6.12. Difference maps showing the expansion and reduction in area occupied by barren ground and the percent change for the classified time period.

6.4 Human Induced Land Cover Change

6.4.1 Changes in Built Up Areas

Areas of development and areas that have reverted back to a more natural state are important to observe, as these have significant implications for their underlying ground thermal regimes. The city of Igarka showed the most drastic change over the observed time period, shrinking by 4.1km^2 (Figure 6.13). The city's contraction was due to the closing of the lumber mill that supported the monotown until 2000. The drastic out-migration was partially encouraged by official programs in an attempt to resettle dependent citizens in more prosperous regions of Russia, and to condense the town's population and resources in the newer and safer buildings in the western half of the settlement (Parente et al., 2012).

Many of the traditional wooden buildings in the historic sections of town were not built in such a way that could compensate for differential thaw like the later Soviet era foundations were designed to, leaving them subject to extreme deformations due to differential thaw (Davis, 2001). Personal communications with residents and regional experts explain that these sections of the town were abandoned and eventually razed or burned (Figure 6.14.a).

The rapid clearing of the historic town center, particularly those areas that were burned, facilitated vegetation reclamation. First colonizers are species such as fireweed (*Chamerion angustifolium*), and tussock cottongrass (*Eriophorum vaginatum*). These are then followed by larger and denser shrub species and trees such as alders (*Alnus fruticosa*), and silver birch (*Betula pendula*), (e.g. Abaimov & Sofronov 1996, Racine et al. 2004, Tchebakova et al. 2009, Walck et al. 2011) (Figure 6.14.b). As the Igarkan

population continues to decline it is likely that this vegetative encroachment and infilling into the abandoned eastern portions of the city will continue.

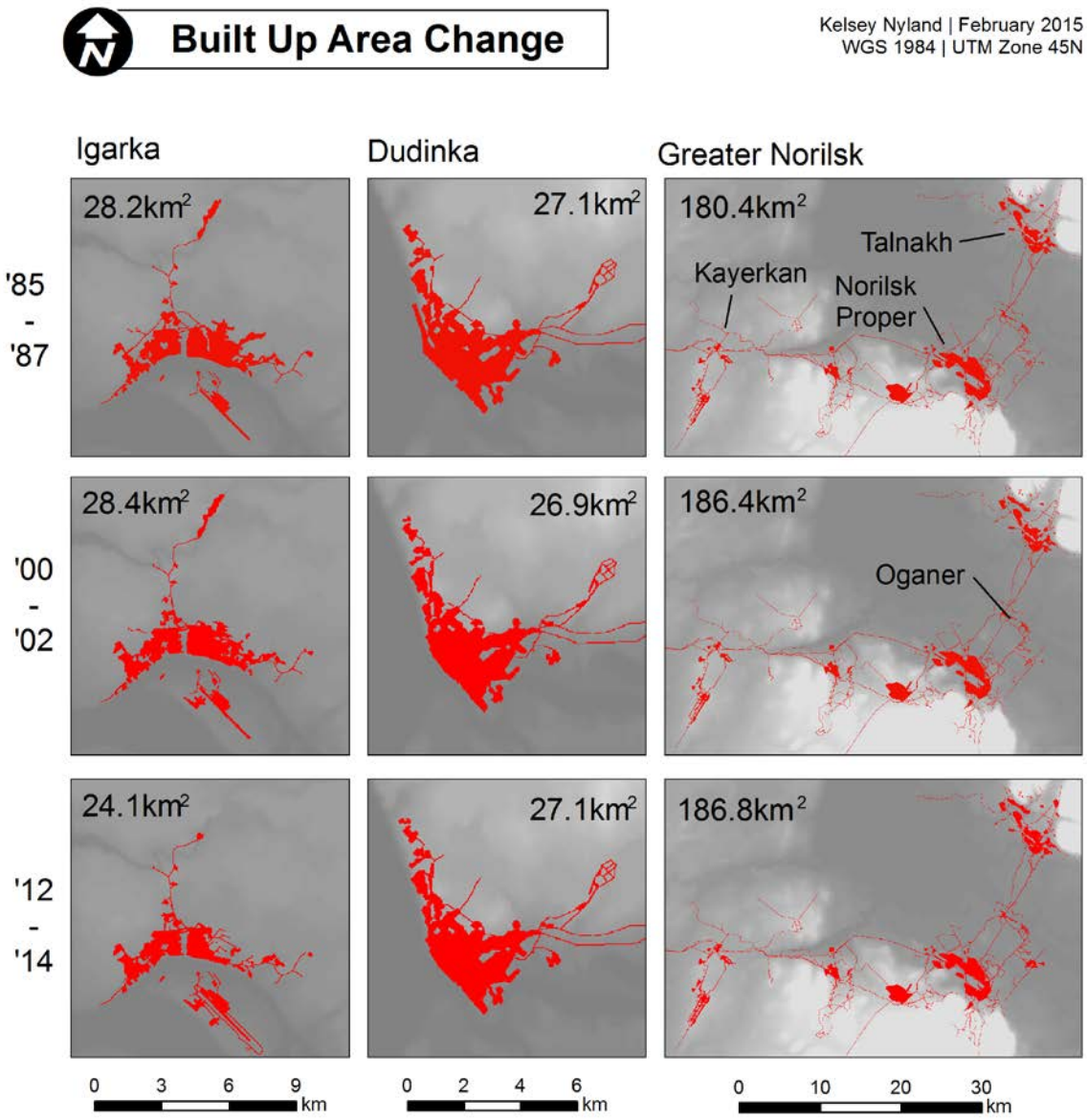

Figure 6.13. Total area occupied by the cities of Igarka, Dudinka, and Greater Norilsk, throughout the time period. Note that Igarka has undergone the most drastic changes reducing in size by 4.1km^2 or14.5%. Also, the only development in the Greater Norilsk area was the construction of Oganer, a satellite community left unfinished.

Figure 6.14. Photos facing north on Kirova Street in Igarka, Russia. Note a) the sloping roofs indicating deformations in photo a taken in 1966 (photo courtesy of N. Tananaev), and in photo b) the replacement by vegetation in 2011 after much of the infrastructure had been removed (photo by author).

Meanwhile, the built up areas of Dudinka did not change significantly, but Norilsk continued to develop marginally until the dissolution of the Soviet Union. The last development in the Greater Norilsk region was the satellite settlement of Oganer. Its construction began in 1986 to accommodate expected increases in population as existing residential housing in Norilsk proper and the satellite towns of Kayerkan and Talnakh had already been exhausted. The downward economic turn experienced in the early 1990s caused the city planners to slow and scale back the planned construction. It was eventually halted altogether in 1994 (Grebenets, personal communications, July 2014). While the 14-story state-of-the-art hospital in Oganer was finished and is currently operational, the new settlement was left largely unfinished, with partially constructed multistory buildings on gravel pads composing the majority of the 6km^2 gain in built up area between the mid-1980s and early 2000s.

The significant reinvestment in the city of Norilsk in recent years can be attributed to the success of Norilsk Nickel MMC, but this socio-economic change cannot be related to the urban aerial extent, as it has not manifested itself through lateral expansion. Revealed during initial field work in Norilsk, the reinvestment in the urban infrastructure has taken on the unique morphologic trend of vertical cycling. The foundations, specially constructed for permafrost conditions, are recycled. Older and heavier concrete and steel construction materials used in the original Soviet prefabricated buildings are cleared off and the foundation is allowed to refreeze without added weight and is then used for a new building using lighter materials such as corrugate metals (Kerimov et al., 2014). This vertical urban morphologic cycling presents problems for identifying urban patterns of development / growth and decay as they will not be picked

up through satellite image classification as they are elsewhere in the world. However, this does present an intriguing method for permafrost management in the Arctic urban context.

6.5 Case Studies of Natural and Anthropogenic Land Cover Change Forcings

In order to isolate some of the causes of the spatial and temporal trends noted in the classified land covers previously discussed for the larger study area, three 50km^2 case study areas were established within the scene (Figure 5.15). Case study number one represents an area not directly impacted by anthropogenic activities. It is located approximately 100km North-northeast of the Norilsk city proper, covering the escarpment between the lacustrine valley and the Putorana Plateau. This location captures the variety of topography and also places the study area outside of the severe to moderate pollution zones emitted from the Norilsk mining and metallurgy activities. While the pollution boundaries are not well defined, this area maintains its lichen covers and vegetative metal content is at or near natural levels (Vlasova et al. 1992, Zubareva et al. 2003, AMAP 2010, Baklanov et al. 2012). The other two case study areas represent those that are directly affected by the industrial activities and are both situated within the maximum pollution zone (Vlasova et al. 1992, AMAP 2010, Baklanov et al. 2012). Case study number two is situated so that it includes the entire Greater Norilsk administrative district, including its industrial complex. Case study number three is located to the southeast of the city in the direct path of the prevailing northwest winds that blow the cities pollution through the valley (Walter et al., 2012).

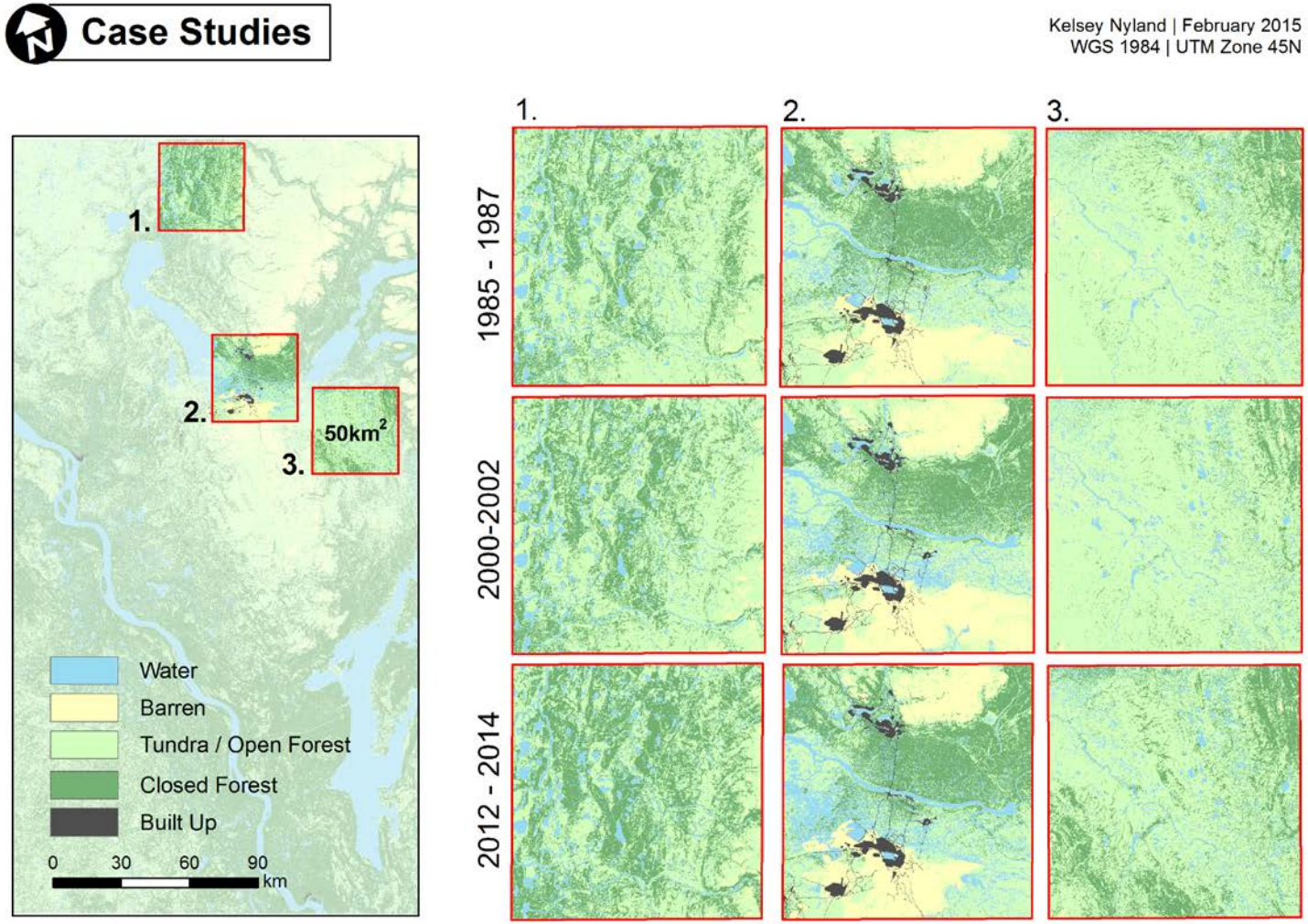

Figure 6.15. Difference maps showing the expansion and reduction in area occupied by barren ground in the Lower Yenisei for the three classified time periods.

Observing the changes in the proportions of area occupied by the different land covers within each of these three case study areas reveals some of the distinct forcing trends discussed in the previous sections as forced by changes in regional climate. Within the first case study area (Figure 6.16.a), there is a general infilling of vegetation, part of the general northward encroachment of taller vegetation throughout the Arctic. The rising altitudinal treeline can also be observed again here as the first case study's topography increases from east to west. Along the western edge of the area, the barren ground at higher elevations is replaced by tundra / open forests, followed by closed forests.

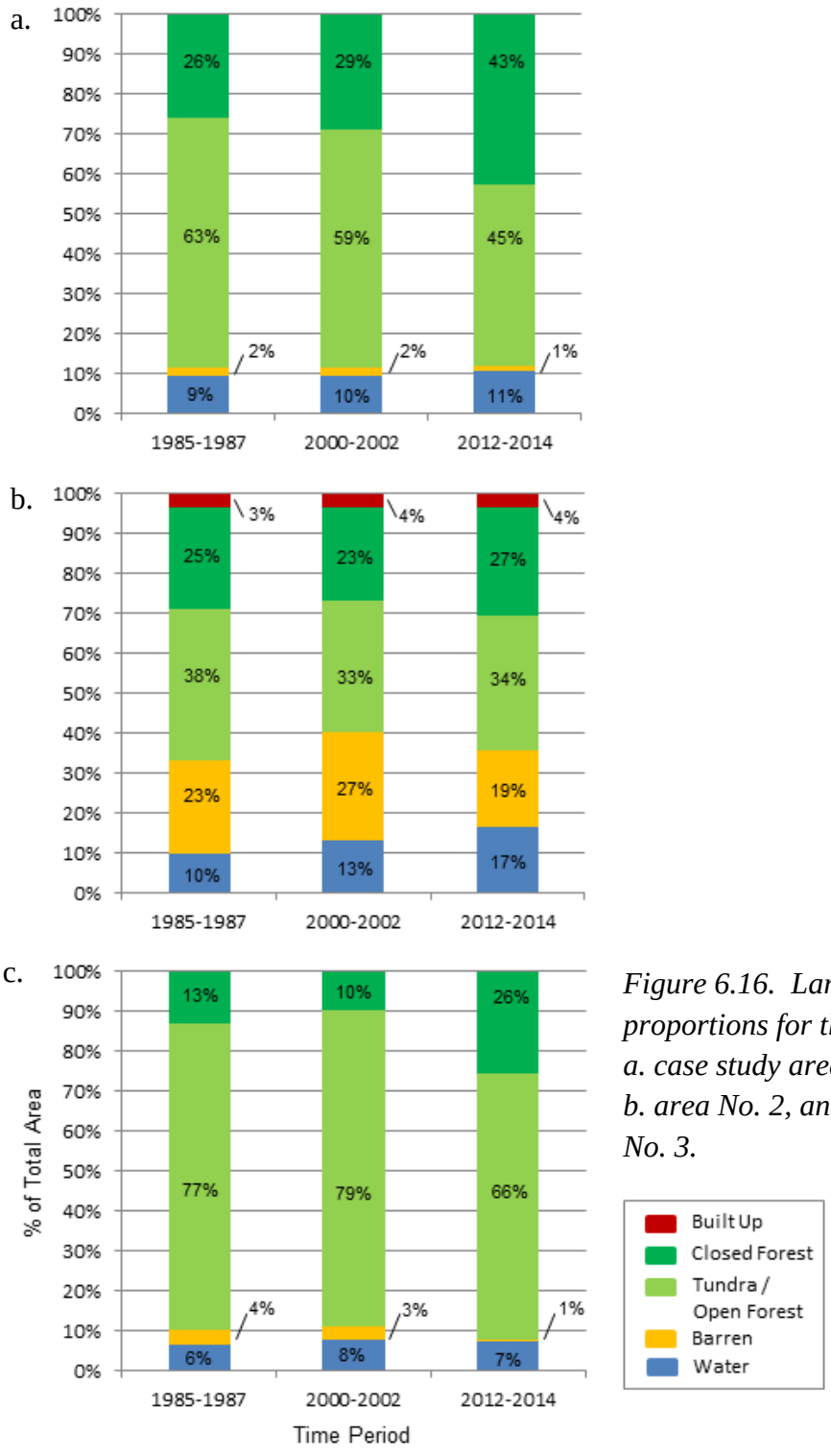

Figure 6.16. Land cover proportions for the 50km^2 a. case study area No. 1, b. area No. 2, and c. area No. 3.

The land cover progressions in the second and third case studies however are driven by the compounded effects of climate forcing and intensive anthropogenic activity. Within this area there is an initial decrease in forest and tundra cover to the southeast of Norilsk and replaced by barren ground. This is followed by an eventual rebounding of the vegetative land covers in the barren areas (Figure 6.16.b-c). This is typical of pollutant emissions from a point source borne by the prevailing winds which in this case come from the northeast (Vlasova et al. 1992, Zubareva et al. 2003, AMAP 2010, Walter et al. 2012). This observed process is likely one of secondary plant succession, where the zone to the southeast of Norilsk quickly transitions to barren ground and then is reclaimed by tundra / open forest covers, following the changes in annual emissions produced by the smelting operations in the Norilsk industrial complex (Figure 6.17). Secondary plant succession being the process where there is an initial disturbance that reduces the extent of a previously established vegetative complex and is then replaced by species that can resist the previously inhibiting growth factor (Horn, 1974), in the case of Norilsk, SO_2 laden pollution.

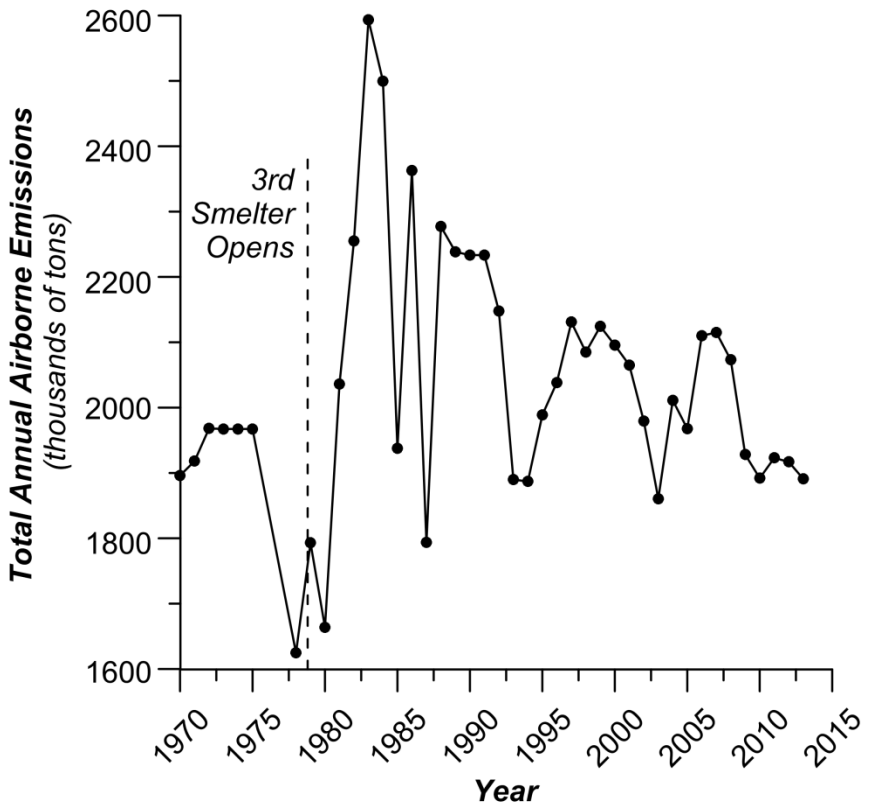

Figure 6.17. Total annual airborne emissions (sum of total SO_2 and particulate emissions) from smelter factories in Norilsk. The sharp increase in emissions in the early 1980s is attributable to the opening of the third smelter, Nadezhda, in 1979. Source: Norilsk Nickel Annual Reports and Kozlov et al. 2009.

The third and largest smelting factory, called *Nadezhda,* began operation in 1979. Following this, the total sulfur dioxide (SO_2) and particulate emissions nearly tripled. Sulfur dioxide, being the greatest component of the airborne emissions (>95% every year) and heavy metal emissions from the Norilsk Nickel smelters damage plant tissues and acidify and leech nutrients from the soils eventually killing large swaths of larch forest stands (Vlasova et al. 1992, AMAP 2010). This reduced closed forest cover seen in the transition between the classifications from the mid-1980s and early 2000s as more

of the understory is exposed and therefore classified as tundra or open forest and in the more devastated areas as barren ground.

By the early 1990's the vegetative damage to the southeast of Norilsk was described as "total vegetative damage" (AMAP, 2010) and "catastrophic damage" (Vlasova et al., 1992). Lichens are extremely vulnerable to pollutants along with other native species including larch trees (*Larix gemelinii*), Siberian spruces (*Picea obovata*), marsh labrador tea (*Ledum palustre*), and woolly willows (*Salix lanata*) (Vlasova et al., 1992). In a plot study conducted in July 2002, the occurrences of vascular plant species with increasing distance from the smelting factories were surveyed and researchers found that the numerous species were present in the closest plots (2.5 km). These species include dwarf birch (*Betula nana*), Siberian alder (*Duschekia fruticosa*), willows (*Salix recurvigemmis*), blueberries (*Vaccinium uliginosum*), horsetail grass (*Equisetum* sp.), and various grasses (*Poa* spp.) (Kozlov et al., 2009). It is therefore likely that the infilling trend causing the transition from open forest to closed forests observed by Kirdyanov et al. (2012) is similar to what is occurring within the severely polluted zone. Where the taller canopy of the original larch forests was killed off and opened the area to the succession of more pollutant resistant species, such as those documented by Kozlov et al. (2009). The colonizing species that are able to survive despite the high levels of SO_2, particulates, and heavy metals, continued to fill in the area until they were dense enough to be captured at the 30m resolution of Landsat in the second half of the classified time period.

Far more research has been conducted in the Fennoscandia region that confirms this theory of Arctic flora succession in SO_2 and heavy metal polluted areas. These

studies focus on land cover changes due to emissions originating from smelters in Nikel and Zapolyarnyy, Russia which are also a production division of Norilsk Nickel. Here, emissions cross the border into Finland and Norway where they have triggered similar plant succession processes (e.g. Høgda et al. 1995, Tømmervik et al. 1995, AMAP 2010). These studies found that where initially pollution had decimated tree cover and ground vegetation, several native shrub species such as crow berries (*Empetrum nigrum* ssp.) (Bakkal 1992, Tømmervik 1995), bilberrys (*Vaccinium myrtillus*), and grasses (*Poa* ssp.) (Deyeva & Maznaya 1993, Tømmervik 1995) all increased within the severely polluted zones (AMAP 2010).

The changes to waterbodies with these two anthropogenic-impacted case studies are also largely to do with changes in the local industry. For example, the mining and metallurgical industry uses large waste retention and recycling systems such as those identified within the Greater Norilsk region. Figure 6.18 shows two examples of large lakes located within the second case study that are being artificially created to hold more industrial waste and another being drained. These waterbodies are also heated from their use in mining and smelting processes in addition to the large thermal capacity of water have serious impacts on the underlying ground thermal regime.

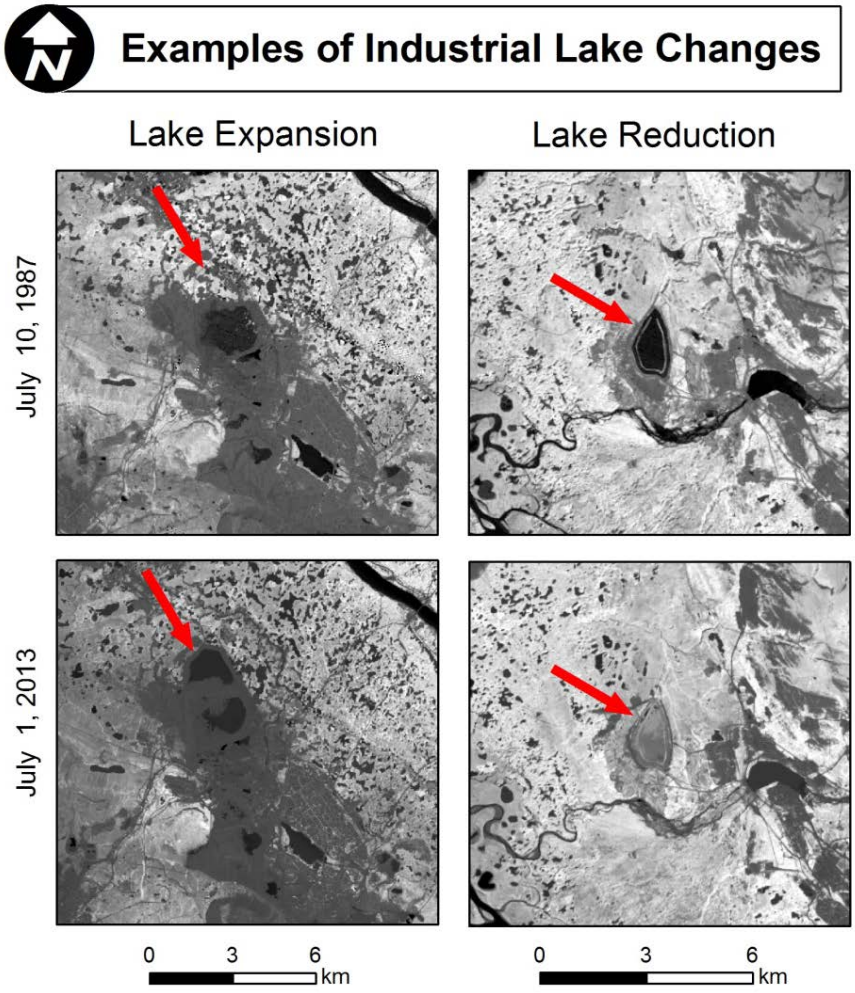

Figure 6.18. Examples of lake changes within built up areas taken from original Landsat scenes displayed in grey scale. The two left hand images are of the industrial waste lakes in Norilsk and the two right hand images are of the industrial aeration lake in the Norilsk satellite settlement of Talnakh.

6.6 Implications for the Permafrost System

6.6.1 Climate-induced Changes

The warming atmosphere and increased climatic signal acting on the ground surface propogates downward, thawing permafrost (Romanovsky et al., 2010). The increased precipitation particularly, in the form of snow, is another factor that can significantly alter the climatic signals. The relatively low thermal conductivity of snow is what makes it such a good insulator for underlying soils. Therefore, increased snow accumulation can maintain a much warmer ground thermal regime through winter as compared to soils without snow cover that would cool rapidly, promoting permafrost agradation (Stieglitz et al. 2003, Ishikawa 2003).

As previously discussed, a number of studies found that increases in large lake area can indicate permafrost degradation within the continuous permafrost zone, while lake reductions are found in discontinuous permafrost areas (e.g. Yoshikawa & Hinzman 2003, Smith et al. 2005, Karlsson et al. 2014). However, the spatial distribution of large lake changes documented within this time series does not appear to correlate with any defined permafrost zones, such as those portrayed on the Circumpolar map by Brown et al. (1998) as it has in previous studies (e.g. Yoshikawa & Hinzman 2003, Smith et al. 2005). Though, this map has been found to be too coarse and poorly defined for regional high resolution lake studies (Smith et al., 2007, Karlsson et al. 2014). Even using the more detailed permafrost map by Yershov et al. (1991), no significant patterns could be discerned that correlate lake change with permafrost continuity. Although, the southernmost portions of the study area, defined as discontinuous by Yershov et al., are

still made up of a high percentage of permafrost (underlying 80% of the area). Therefore, the areas where lakes are shrinking and disappearing are likely indicators of the presence of taliks that are expanding (areas of unfrozen ground). Where taliks provide significantly more storage for ground water to drain into causing lakes to shrink and eventually disappear (French 2007 p. 136 – 140, Muskett & Romanovsky 2011).

Another indicator of general permafrost warming and degradation throughout the study area is the expansion of larger shrubs and trees facilitated by an increasing active-layer thickness. A thicker active-layer can support larger root systems and is therefore a primary factor that allows for larger shrub and tree complexes to expand their territory in this region (Myers-Smith et al., 2011), causing the observed transition to more closed forests. The increased thickness of the vegetation layer, as well as the accompanying thicker organic soil layer on the ground surface, can provide more thermal insulation mitigating the summer climate signal (e.g. French 2007, Pearson et al., 2013). However, this increased insulation also acts to mitigate the winter cooling signal as well, maintaining a warmer ground thermal regime than that with less vegetative cover, thus preventing permafrost aggradation (e.g. Walker et al. 2003, Kelley et al. 2004, Instanes et al. 2005). Along with the drastic increases in air temperature that are projected to continue, this 'greening trend' will likely persist (IPCC, 2013).

6.6.2 Anthropogenic-Induced Changes

Built up areas and the anthropogenic activities that occur there produce heat and remove protective vegetation both of which are detrimental to underlying permafrost. Due to drastic population reduction and abandoned infrastructure, anthropogenic activity

that warms the ground has largely ceased in the abandoned areas of Igarka. In re-vegetated areas, such as the historical section of Igarka, this does not necessarily imply that the permafrost ceases to degrade as mean annual air temperatures that continue to rise.

Also, in the industrialized areas, such as within the Norilsk industrial complex, many of the changes in surface hydrology were purposeful and made for industrial processes rather than from ground thaw. Therefore, these changes cannot be strictly interpreted as indications of permafrost degradation, but instead as areas that will likely cause degradation. For instance, artificial lake development will likely cause permafrost thaw by promoting the formation of a talik beneath due to the high thermal capacity and temperature of the water (Williams & Smith 1989, French 2007). Conversely, lake drainage facilitates freezing and permafrost aggradation. This was well documented in similarly long-term artificially-drained lake experiment in Barrow, Alaska (Mackay 1997, French 2007).

Lastly, the secondary plant succession process caused by the pollution from the Norilsk Nickel smelting operations also poses some interesting implications for ground temperatures. The initial disturbance which killed and removed much of the vegetation and established the industrial barrens to the southeast of Norilsk could have allowed for significantly more of the atmospheric cold signal in winter to penetrate much deeper into the ground (Williams & Smith 1989, French 2007). However, in the midst of a warming climate, vegetation was able not only to eventually reclaim significant portions of the industrial barrens, but also transition to larger and denser species complexes indicative of a thickening active layer.

Chapter 7: Conclusions

7.1 Summary of Results

Climatic changes are occurring at a rapid and drastic rate within the Lower Yenisei River region. Based on NASA-MERRA data this work has found that mean annual air temperatures have increased over the last 30 years by 1.22°C at an average rate of 0.05°C/year, while mean total annual precipitation has decreased by 16.45mm. Of that, the mean maximum annual snow depth has decreased on average by 0.104m. These climatic changes provoke a number of environmental changes, triggering feedback mechanisms that further contribute to the regional climate warming and environmental change.

Using a new classification methodology, Landsat dense time stacking, a number of thresholds were applied to all avaliable data, NDVI products, and a DEM to classify several landcover types that could be identified at the Landsat 30m resolution. This methodology proved sucessful, yeilding a final map series covering 29 years with acceptable accuracies for each classified map.

Within the classified area the area occupied by closed system, large lakes had increased by 0.92% (190.27km^2). Those in southern portions of the scene have also decreased by 0.39% (80.56km^2) in certain areas. These are indicative of permafrost degredation within the continuous zone of permafrost. The minority of lakes that were observed as shrinking or dissappearing all together are likely areas occupied by taliks or

were shallow and succumbed to increased evaporative processes and the diminished precipitation.

Two distinct greening trends, both general infilling and a rising tree line, were also observed throughout the observed time period. Where the net change for the area occupied by tundra and open forests over the observed 29-year period was a 6.88% decrease in its area (5720.6km^2). This was also true of barren ground which decreased by 5.71% (696.8km). While in some areas it was the tundra and open forest that took the place of barren ground, it was largely closed forests that expanded into both of these areas, expanding its territory by 9.42% (5874.693km). While permafrost thaw and the consequent deepening of the active layer allows for larger plant root systems to take hold, such as those for large shrubs and trees that make up closed forests, an increased vegetation layer can locally cool the underlying ground thermal regime by offering a thicker insulating layer to mitigate the climate signal in summer (e.g. French 2007, Pearson et al., 2013). However, the inverse of this is the increased insulation in winter maintaining a warmer permafrost condition, preventing aggradation (e.g. Walker et al. 2003, Kelley et al. 2004, Instanes et al. 2005).

The three cities included in the study are indicative of different tracks taken by post-Soviet Siberian cities as indicated by their recent population trends. While there was a general outmigration from Arctic Siberia following the dissolution of the Soviet Union, felt by many communities in the far north, in recent years they have begun to take different tracts illustrated by the three cities included in this study. Igarka, characterized by continued population decline and decaying infrastructure due to cryogenic weathering and permafrost degradation led officials to raze many of their older buildings reducing

the extent of the built up area by nearly 15%. The reduction in anthropogenic activity and conversion of part of the city back to natural covers may have allowed the underlying ground to cool in that area, but this will not be enough to compensate for the rising air temperatures.

Meanwhile the spatial extent of the cities of Dudinka and Norilsk have remained relatively constant, while Dudinka's population has stabilized and Norilsk's has begun to grow slightly since 2010. This recent trend is not reflected in the spatial extent of Norilsk, due to a relatively new and unique morphologic trend of vertical cycling. Large Soviet era building foundations, engineered to withstand permafrost conditions, are being recycled by demolishing the old building being supported and replaced with a building made from newer and lighter materials.

In examining the three case study areas; one in a natural setting north of Norilsk, and the other two encompassing the city and in the middle of the polluted zone, two distinct land cover progressions associated with climatic and anthropogenic forcings were identified. The majority of what has been previously discussed embodies the natural land cover progression, where there is a general increase in the numbers and total area of lakes and there is a general infilling of vegetation causing the transition to more closed forest cover that also includes the rising tree line. The anthropogenic forced land cover progression is proceeded by an initial increase in barren ground due to pollution killing the vegetation downwind of the point source. This initial clearing of area allows for secondary plant succession to occur. Re-vegetation was observed in the later half of the time period for areas inundated by pollution, but the plant community's composition has

likely transitioned to be dominated by those species that are more resilient to the large concentrations of SO_2, particulate matter, and heavy metals.

Based on these conclusions, the initial hypotheses posed that; 1) both climatic and anthropogenic forcings are acting on land covers in the Lower Yenisei River region; and the areas that they impact are distinct, and 2) that socio-economic factors trigger growth or decay of urban settlements in the Russian Arctic, putting significant stress on the surrounding environment. In the presence of climate change this can potentially intensify permafrost warming and degradation, can both be accepted.

7.2 Suggestions for future Research

Since the new Landsat dense time stacking methodology has proved successful in the Lower Yenisei it could be applied to other regions of the Arctic. Ways to improve this method would be to find ways to increase the numbers of images included in the stacks. Denser stacks would provide more information for the classification decisions to be based on producing a more thorough and accurate map product. This could be accomplished through finding additional imagery or increasing the numbers of calculated layers added to the stacks, such as the normalized difference water index (Gao, 1996), or spatial features (Graesser et al., 2012). Future use of this method may also consider applying it to dense stacks of high resolution imagery for more detailed and site specific investigations. Though it make may take significant time before there is enough repeat imagery of particular areas within the Arctic to establish an adequate time series to perform this type of analysis at high resolution.

For this work *a piori* data was available both from several summers of field experience in the region on the International Permafrost Field Course and from regional dendrochronology and phonologic studies. Future studies, if conducted with less ground knowledge should consider the use of machine learning for better decision making during classification. They might consider algorithms such as the decision tree (Schneider 2012, Chasmer et al. 2014) or random forest ensemble learning method (Rodrígues-Galiano et al. 2012).

Additional directions for work based on the results presented here might include *in situ* vegetation plot studies in an effort to validate the previously speculated different forcings (climatic and anthropogenic) that are impacting land cover changes with distance from these developed areas in the Lower Yenisei. Such studies might attempt to recreate the plots that were used for surveying in 2002 by the point source pollution project (Kozlov et al., 2009) and the altitudinal transect used by the forestry project in the Putorana Mountains that documented the infilling of large shrubs and woody plants (Kirdyanov et al., 2012). Monitoring sites should observe the vegetative covers as well as monitor near surface permafrost parameters such as the Circumpolar Active Layer Monitoring program's flux plot study does in the Alaskan Arctic (Klene et al., 2001, Shiklomanov et al. 2008, Nyland et al. 2012).

References

ACIA [Arctic Climate Impact Assessment]. 2004. *Impacts of a warming Arctic: Arctic climate impact assessment*. Cambridge University Press, Cambridge, UK.

Abaimov, A.P., Sofronov, M.A. 1996. The Main Trends of Post-Fire Succession in Near-Tundra Forests of Central Siberia. *Fire in Ecosystems of Boreal Eurasia, Forestry Sciences*, 48: 372 – 386.

AMAP [Arctic Monitoring and Assessment Programme]. 1998. Arctic pollution issues: a state of the Arctic environment report. In *Arctic Monitoring and Assessment Programme (AMAP)*, Oslo, Norway.

AMAP [Arctic Monitoring and Assessment Programme]. 2002. Arctic pollution 2002: persistent organic pollutants, heavy metals, radioactivity, human health, changing pathways. In *Arctic Monitoring and Assessment Programme (AMAP)*, Oslo, Norway.

Anoklin, A., Kuznetsov, S., Lachinonskii, S. 2014. A Spatial Study of Geo-Economic Risk Exposure of Russia's Arctic Mono-Towns with Commodity Export-Based Economy. *Journal of Geography and Geology*, 6 (1): 38 – 45.

Auerbach, N.A., Walker, D.A. 1997. Effects of roadside disturbance on substrate and vegetation properties in arctic tundra. *Ecological Applications*, 7(1): 218-235.

Bakkal, I.J., 1992. The state of the field layer in polluted and unpolluted scots pine forests in the Kola Peninsula. In: B. Sivertsen (ed.). Air pollution problems in the Northern Region os Fennoscandia included Kola. In *Proceedings from the Seminar at Svanvik, Norway*, 1 – 3 June 1993. Norwegian Institute for Air Research, Lillestrøm, NILU TR 14/94, 0-8976.

Baklanov, A.A., Penenko, V.V., Mahura, A.G., Vinogradova, A.A., Elansky, N.F., Tsvetova, E.A., Rigina, O.Y. ... Zakey, A. 2012. Aspects of Atmospheric Pollution in Siberia. In: P.Y. Groisman, G. Gutman (eds.). *Regional Environmental Changes in Siberia and their global consequences*. Springer.

Bekryaev, R.V., Polyakov, I.V., Alexeev, V.A., 2010. Role of polar amplification in longterm surface air temperature variations and modern Arctic warming. J. *Climate*, 23, 3888–3906.

Bergen, K.M., Hitztaler, S.K., Kharuk, V.I., Krankina, O.N., Loboda, T.V., Zhao, T., Shugart, H.H., Sun, G. 2012. Human dimensions of environmental change in Siberia. In: P.Y. Groisman, G. Gutman (eds.). *Regional Environmental Changes in Siberia and their global consequences*. Springer.

Bishop, Y., Fienberg, S., Holland, P. 1975. *Discrete Multivariate Analysis: Theory and Practice*. MIT Press, Cambridge, MA. 575 pp.

Blinnikov, M.S. 2011. *A Geography of Russia and Its Neighbors*. New York, New York: The Guilford Press. Print.

Blok, D., Sass-Klaassen, U., Schaepman-Strub, G., Heijmans, M.M.P.D., Sauren, P., Berendse, F. 2011. What are the main climate drivers for shrub growth in Northeastern Siberian tundra? *Biogeosciences*, 8: 1169 – 1179, doi: 10.5194/bg-8-1169-2011.

Bosilovich, M.G. 2008. NASA's modern era retrospective-analysis for research and applications: Integrating Earth observations. *Earthzine*, posted 26 September 2008. http://www.earthzine.org/2008/09/26/nasa-modern-era-retrospective-analysis/.

Brown, J., Ferrians, O., Heginbottom, J.A., Melnikov, E. 1998. *Circum-Arctic Map of Permafrost and Ground-Ice Conditions*. Boulder, Colorado USA. National Snow and Ice Data Center.

Chapin, F. S., et al. (2005), Role of land-surface changes in Arctic summer warming, *Science*, 310, 657–660.

Chasmer, L., Hopkinson, C., Veness, T., Wuinton, W., Baltzer, J. 2014. A decision-tree classification for low-lying complex land cover types within the zone of discontinuous permafrost. *Remote Sensing of the Environment*, 143: 73 – 84.

Chen, M., Rowland, J.C., Wilson, C.J., Altmann, G.L., Brumby, S.P. 2013. The Importance of Natural Variability in Lake Areas on the Detection of Permafrost Degradation: A Case Study in the Yukon Flats, Alaska. *Permafrost and Periglacial Processes*, 24: 224 – 240, doi: 10.1002/ppp.1783.

Congalton, R.G., Green, K. 2008. *Assessing the Accuracy of Remotely Sensed Data: Principles and Practices*, 2nd edn., CRC Press, Boca Raton, Florida, Print.

Davis, N. 2001. *Permafrost: A Guide to Frozen Ground in Transition*. University of Alaska Press, Fairbanks, 213 – 229p.

Derksen, C., Brown, R., Mudryk, L., Luojus, K. 2014. Terrestrial Snow Cover. In *Arctic Report Card 2014*, http://www.arctic.noaa.gov/reportcard.

Derome, J., Lukina, N. 2011. Environmental pollution and land-cover/land-use change in arctic areas. In: Gutman, G., Reissell, A. (eds) *Eurasian arctic land use and land cover in a changing climate*. Springer, Dordrecht, pp 269 – 289.

Deyeva, N.M., Maznaya, E.A.. 1993. The state of the bilberry in an unpolluted forest of the Kola peninsula. *In:* M.V. Kozlov, E. Haukioja and V.T. Yarmishko (eds.). *Aerial pollution in Kola Peninsula. Proceedings of an International workshop*, April 14-16, 1992, St. Petersburg, Russia, pp. 308-311. University of Turku, Department of Biology, Laboratory of Ecological Zoology, Finland.

Fedorov, A.N., Ivanova, R.N., Park, H., Hiyama, T., Iijima, Y. 2014. Recent air temperature changes in the permafrost landscapes of northeastern Eurasia, *Polar Science*, 8 (2): 114 - 128.

Ferranti, J., Hormann, C. (2012, November 1). DEM Coverage Map. In *Viewfinder Panoramas*. Retrieved January 14, 2015, from http://www.viewfinderpanoramas.org/dem3.html#eurasia

Foody, G.M, 2002. Status of land cover classification accuracy assessment. *Remote Sensing of Environment*, 80: 185 – 201.

Forbes, B.C., Fauria, M.M., Zetterberg, P. 2010. Russian Arctic warming and 'greening' are closely tracked by tundra shrub willows. *Global Change Biology*, 16: 1542 – 1554.

French, H.M. 2007. *The Periglacial Environment*. Wiley.

Friedman, S.Z., Angelici, G. 1979. The detection of urban expansion from Landsat imagery. *Remote Sensing Quarterly*, 1: 58-79.

Frost, G.V., Epstein, H.E. 2014. Tall shrub and tree expansion in Siberian tundra ecotones since the 1960's. Global change biology, 20 (4): 1264 – 1277.

Gao, B. 1996. Anthropogenic Disturbance and Patch Dynamics in Circumpolar Arctic Ecosystems. *Conservation Biology*, 15(4): 954-969.

Goetz, S.J., Epstein, H.E., Alcaraz, J.D., Beck, P.S.A., Bhatt, U.S., Bunn, A., Comiso, J.C., Jia, G.J., Kaplan, J.O., Lilschke, H., Lloyd, A., Walker, D.A., Yu, Q. 2011. Recent changes in Arctic vegetation: Satellite observations and simulation model predictions. *Eurasian Arctic Land Cover and Land Use in a Changing Climate. Springer*. New York.VI pp. 9-36.

Graesser, J., Cheriyadat, A., Vatsavai, R.R., Chandola, V., Long, J., Bright, E. 2012. Image based characterization of formal and informal neighborhoods in an urban landscape. Selected Topics in *Applied Earth Observations and Remote Sensing, IEEE Journal of*, 5 (4): 1164 – 1176.

Grebenets, V., Streletskiy, D., Shiklomanov, N. 2012. Geotechnical safety issues in the cities of Polar Regions. *Geography, Environment, Sustainability Journal*, 5(3): 104-119.

Groisman, P.Y., Gutman, G., Shvidenko, A., Gergen, K.M., Baklanov, A.A. 2012. Introduction: Regional Features of Siberia. In: P.Y. Groisman, G. Gutman (eds.). *Regional Environmental Changes in Siberia and their global consequences*. Springer.

Gutman, G., Reissel, A. (eds). 2010. *Eurasian Arctic Land Cover and Land Use in a Changing Climate*. Springer.

Hallinger, M., Manthey, M., and Wilmking, M. 2010. Establishing a missing link: warm summers and winter snow cover promote shrub expansion into alpine tundra in Scandinavia. *New Phytologist*, 186: 890 – 899.

Harsch, M.A., Hulme, P.E., McGlone, M.S., Duncan, R.P. 2009. Are treelines advancing? A global meta-analysis of treeeline response to climate warming. *Ecology Letters*, 12: 1040 – 1049.

Heleniak, T. 2009. Growth Poles and Ghost Towns in the Russian Far North. In *Russia and the North*, edited by E.W. Rowe, 129–162. Ottawa: The University of Ottawa Press.

Hill, F., Gaddy, C. 2003. *The Siberian Curse: How Communist Planners Left Russia Out in the Cold*. Washington, DC: Brookings Institution Press, Print.

Hinzman, L.D., Deal, C.J., McGuire, A.D., Mernild, S.H., Polyakov, I.V., Walsh, J.E. 2013. Trajectory of the Arctic as an integrated system. *Ecological Applications*, 23: 1837 – 1868.

Høgda, K.A., Tømmervik, H., Solheim, I., Marhung, Ø. 1995. Use of multitemporal Landsat image data for mapping the effects from air pollution in the Kirkenes-Pechenga area in the period 1973-1994. *Norut Report*, University of Tromsø, IT2039/1-95.

Ho, J. 2010. The implications of Arctic sea ice decline on shipping. *Marine Policy*, 34: 713 – 715.

Horn, H.S. 1974. The ecology of secondary succession. *Annual Review of Ecology, Evolution, and Systematics*, 5: 25 – 37.

Instanes, A., Anisimov, O., Bringham, L., Goering, D., Khrustalev, L.N., Ladanyi, B., Otto Larsen, J. 2005. Infrastructure: buildings, support systems, and industrial facilities. In: Symon, C., Arris, L., Heal., B (Eds.) *Arctic Climate Impact Assessment*. Cambridge University Press, Cambridge.

Intergovernmental Panel on Climate Change (IPCC). 2013. *Climate Change 2013: The Physical Science Basis, Contribution of Working Group I to the Fifth Assessment*

Report of the Intergovernmental Panel on Climate Change. Stocker, T.F., Qin, D., Plattner, G.K., Tignor, M., Allen, S.K., Boschung, J., ... Midgley, B.M. (Eds.) Cambridge University Press, Cambridge.

Ishikawa, M. 2003. Thermal response at the snow-ground interface and their implications for permafrost investigation. *Geomorphology*, 52: 105 – 120.

Jia, G.J., Epstein, H.E., Walker, A.D. 2003. Greening of arctic Alaska, 1981-2001. *Geophysical Research Letters*, 30(20):2067.

Karlsson, J.M., Lyon, S.W., Destouni, G. 2012. Thermokarst lake, hydrological flow and water balance indicators of permafrost change in Western Siberia. *Journal of Hydrology*, 464 – 465: 459 – 466.

Karlsson, J.M., Lyon, S.W., Destouni, G. 2014. Temporal Behavior of Lake Size-Distribution in a Thawing Permafrost Landscape in Northwestern Siberia. *Remote Sensing*, 6: 621 – 636, doi: 10.3390/rs601621.

Kelley, A.M., Epstein, H.E., Walker, D.A. 2004. Role of vegetation and climate in permafrost active layer depth in the Arctic tundra of northern Alaska and Canada. *Journal of Glaciology and Geocryology*, 26: 269 – 274.

Kennedy, R.E., Cohen, W.B., Schroeder, T.A. 2007. Trajectory-based change detection for automated characterization of forest disturbance dynamics. *Remote Sensing of Environment*, 110:370-386.

Kerimov A.G., Grebenets V.I., Streletskiy D.A., Shiklomanov N.I., Nyland K.E. 2014. Evolution of permafrost landscapes under technogenic impacts. *AGU 2014 Annual Meeting*, San Francisco.

Kharuk, V.I. 2000. Air pollution impact on subarctic forests at Norilsk, Siberia. In: Innes, J.L., Oleksyn, J. (eds) *Forest dynamics in heavily polluted regions*. CAB International, Wallingford, pp. 77 – 86.

Kharuk, V.I., Ranson, K.J., Im, S.N., Naurzbaev, M.M. 2006. Forest-tundra larch forests and climatic trends. *Russian Journal of Ecology*, 37: 291 – 298.

Khon, V.C., Mokhov, I.I., Latif, M., Semenov, V.A., Park, W. 2010. Perspectives of Northern Sea Route and Northwest Passage in the twenty-first century. *Climatic Change*, 100: 757 – 768, doi: 10.1007/s10584-009-9683-2.

Kirdyanov, A. V., Hagedorn, F., Knorre, A.A., Fedotova, E.V., Vaganov, E.A., Naurzbaev, M.M., Moiseev, P.A., Rigling, A. 2012. 20th century tree-line advance and vegetation changes along an altitudinal transect in the Putorana Mountains, northern Siberia. *Boreas*, 41: 56–67. doi: 10.1111/j.1502-3885.2011.00214.x

Klene, A.E., Nelson, F.E., Shiklomanov, N.I., and Hinkel, K.M. 2001. The n-factor in natural landscape: Variability of air and soil- surface temperatures, Kuparuk River basin, Alaska, USA. *Arctic, Antarctic, and Alpine Research*, 33(2): 140-148.

Klene, A.E., Nelson, F.E., Hinkel, K.M. 2013. Urban-rural contrasts in summer soil-surface temperature and active-layer thickness, Barrow Alaska, USA. *Polar Geography*, 36 (3): 183 – 201.

Kozlov, M.V., Zvereva, E.L. 2007. Industrial barrens: extreme habitats created by non-ferrous metallurgy. *Reviews in Environmental Science and Biotechnology*, 6: 233 – 259.

Kozlov, M.V., Zvereva, E.L., Zverev, V.E. 2009. *Impacts of point polluters on terrestrial biota: comparative analysis of 18 contaminated areas*. Springer, Dordrecht.

Kryukova, E.M., Vetrova, E.A., Maloletko, A.N., Kaurova, O.V., Dusenko, S.V. 2015. Socio-Economic Problems of Russian Mono-Towns. *Asian Social Science*, 11 (1): 258 – 267.

Kumpula, T., Pajunen, A., Kaarlejärvi, E., Forbes, B.C., Stammler, F. 2011. Land Use and Land Cover Change in Arctic Russia: Ecological and Social Implications of Industrial Development. *Global Environmental Change*, 21 (2): 550 – 562, doi: 10.1016/gloenvcha.2010.12.010.

Lloyd, A.H. 2005. Ecological histories from Alaskan tree lines provide insight into future change. *Ecology*, 86: 1687 – 1695.

Lindsay, R., Wensnahan, M., Schweiger, A., Zhang, J. 2014. Evaluation of Seven Different Atmospheric Reanalysis Products in the Arctic. *Journal of Climate*, *27*(7): 2588-2606.

Macias-Fauria, M., Forbes, B.C., Zetterberg, P., Kumpula, T. 2012. Eurasian Arctic greening reveals teleconnections and the potential for structurally novel ecosystems. *Nature Climate Change*, 2: 613 – 618.

Mackay, J.R. 1997. A full-scale field experiment (1978 – 1995) on the growth of permafrost by means of lake drainage: a long-term field study. *Géographie physique et Quaternaire*, 52:271 – 323.

Myers-Smith, I., Hik, D., Kennedy, C., Cooley, D., Johnstone, J. Kennedy, A., Krebs, C. 2011 . Expansion of canopy-forming willows over the twentieth century on Herschel Island, Yukon Territory, Canada. *Ambio*, 40: 610 – 623.

Myers-Smith, I.H., Arnesen, B.K., Thompson, R.M., Chapin III, F.S. 2006. Cumulative impacts on Alaskan arctic tundra of a quarter century of road dust. *Ecoscience*, 13, 503–510.

Muller, S. W., 2008: *Frozen in Time: Permafrost and Engineering Problems*. French, H. M., and Nelson, F. E. (eds.). Reston, Virginia: American Society of Civil Engineers. Print.

Muskett, R.R., Romanovsky, V.E. 2011. Alaskan Permafrost Groundwater Storage Changes Derived from GRACE and Ground Measurements. *Remote Sensing*, 3: 378 – 397, doi: 10.3390/rs3020378.

Myers-Smith, I.H., Forbes, B.C., Wilmking, M., Hallinger, M., Lantz, T., Bolk, D., Tape, K.D. … Hik, D.S. 2011. Shrub expansion in tundra ecosystems: Dynamics, impacts and research priorities. *Environmental Research Letters*, 6: 045509, doi: 10.1088/1748-9326/6/4/045509.

Nyland, K.E., Shiklomanov, N.I., Streletskiy, D.A., Klene, A.E., Nelson, F.E. 2012. Effect of Vegetation on Ground Temperature in Northern Alaska. In *Proceedings of the 10th International Conference on Permafrost*, Salekhard, Russia, June 25 – 29, 2012, 1: 295 – 300.

Overland, J., Hanna, E., Hanssen-Bauer, I., Kim, S.J., Walsh, J., Wang, M., Bhatt, U.S. 2014. Air Temperature. In *Arctic Report Card*, http://www.arctic. Noaa.gov/reportcard.

Parente, G., Shiklomanov, N., Streletskiy, D. 2012. Living in the New North: Migration to and from Russian Arctic Cities. *Focus on Geography*, 55 (3):77-89.

Pavlov, A.V. 2006. Current changes of climate and permafrost in the arctic and sub-arctic of Russia. *Permafrost and Periglacial Processes*, 5(2): 101 – 110, doi: 10.1002/ppp.3430050104.

Pearson, R.G., Phillips, S.J., Loranty, M.M., Beck, P.S., Damoulas, T., Knight, S.J., Goetz, S.J. 2013. Shifts in Arctic vegetation and associated feedbacks under climate change. *Nature Climate Change*, 3 (7): 673 – 677.

Peel, M.C., Finlayson, B.L., McMahon, T.A. 2007. Updated world map of the Köppen-Geiger climate classification. *Hydrology and Earth System Sciences*, 11: 1633 – 1644.

Plourde, L., Congalton, R.G. 2003. Sampling method and sample placement: How do they affect the accuracy of remotely sensed maps? *Photogrammetric Engineering and Remote Sensing*, 69: 289 – 297.

Racine, C., Jandt, R., Meyers, C., Dennis, J. 2004. Tundra fire and vegetation change along a hillslope on the Seward Peninsula, Alaska, U.S.A. *Arctic, Antarctic, and Alpine Research*, 36: 1- 10.

Reinecker, M.M., Suarez, M.J., Gelaro, R., Todling, R., Bacmeister, J., Liu, E., Bosilovich, M.G. … Woollen, J. 2011. MERRA: NASA's Modern-Era Retrospective Analysis for Research and Applications. *Journal of Climate*, 24: 3624 – 3517.

Rodrígues-Galiano, V.F., Ghimire, B., Pardo-Igúzqiza, E., Chica-Olmo, M., Congalton, R.G. 2012. Incorporating the downscaled landsat TM thermal band in landcover classification using Random Forest. *Photogrammetric Engineering and Remote Sensing*, 78: 129 – 137.

Romanovsky, V.E., Drozdov, D.S., Oberman, N.G., Malkova, G.V., Khologoc, A.L., Marchenko, S.S., Moskalenko, N.G., Sergeev, D.O., Ukraintseva, N.G., Abramov, A.A., Gilichinsky, D.A., Vasiliev, A.A. 2010. Thermal state of permafrost in Russia. *Permafrost and Periglacial Processes*, 21: 136 – 155.

RosStat. 2015. Russian Federal State Statistics Service. Федеральная служба государственной статистики. "Предварительные итоги Всероссийско переписи населения 2010 года (Preliminary results of the 2010 All-Russian Population Census)" (in Russian). Всероссийская перепись населения 2010 года (All-Russia Population Census of 2010). [www.perepis-2010.ru/results_of_the_census/results-inform.php].

Rouse, J.W., Haas, R.H., Schell, J.A., Deering, D.W. 1974. Monitoring Vegetation Systems in the Great Plains with ERTS. In *Proceedings of the Third Earth resources Technology Satellite-1 Symposium*, Greenbelt: NASA SP-351, 3010-3017.

Schneider, A. 2012. Monitoring land cover change in urban and peri-urban areas using dense time stacks of Landsat satellite data and a data mining approach. *Remote Sensing of Environment*, 124, 689-704.

Schneider von Deimling, T., Meinshausen, M., Levermann, A., Huber, V., Frieler, K., Lawrence, D.M., Huber, V. … Brovkin, V. 2012. Estimating the near-surface permafrost-carbon feedback on global warming. *Biogeosciences*, 9: 649 – 665, doi 10.5194/bg-9-649-2012.

Screen, J.A., Simmonds, I. 2010. The central role of diminishing sea ice in recent Arctic temperature amplification. *Nature*, 464 (7293): 1334 – 1337.

Screen, J.A., Simmonds, I., Deser, C., Robert, T. 2013. The Atmospheric Response to Three Decades of Observed Arctic Sea Ice Loss. *Journal of Climate*, 26.4:1230-1248.

Sejersen, F. 2010. Urbanization, landscape appropriation and climate change in Greenland. *Acta Borealia*, 27 (2): 167 – 188.

Serreze, M. C., Hurst, C. M. 2000. Representation of mean Arctic precipitation from NCEP-NCAR and ERA reanalyses. *Journal of Climate, 13*(1): 182-201.

Shiklomanov, N.I. 2005. From exploration to systematic investigation: Development of geocryology in 19th-and early-20th-century Russia. *Physical Geography*, 26: 249-263.

Shiklomanov, A.I., Lammers, R. 2009. Record Russian river discharge in 2007 and the limits of analysis. *Environmental Research Letters*, 4(4): 045015.

Shiklomanov, N.E., Nelson, F.E., Streletskiy, D.A., Hinkel, K.M., Brown, J. 2008. The Circumpolar Active Layer Monitoring (CALM) Program: Data collection, management, and dissemination strategies. *In Proceedings of the Ninth International Conference on Permafrost*, 29 June – 3 July 2008, Fairbanks, Alaska. 2: 1647 – 1652.

Shiklomanov N.I., and Streletskiy D.A. 2013. Effect of Climate Change on Siberian Infrastructure. In P.Ya. Groisman and G. Gutman (eds.) *Regional Environmental Changes in Siberia and their Global Consequences*. Springer, doi: 10.1007/978-94-007-4569-8_1, 155-170.

Shiyatov, S.G., Terent'ev, M.M, Formin, V.V. 2005. Spatial-temporal dynamics of forest tundra communities in the Polar Ural Mountains. *Russian Journal of Ecology*, 36, 69 – 75.

Smith L.C., Sheng, Y, MacDonald, G.M., Hinzman, L.D. 2005. Disappearing Arctic Lakes. *Science*, 308: 1429.

Smith, L.C., Sheng, Y., and MacDonald, M. 2007. A first pan-Arctic assessment of the influence of glaciation, permafrost, topography and peatlands on northern hemisphere lake distribution. *Permafrost Periglacial Processes*, 18, 201-208, doi: 10.1002/ppp.581.

Smith, L.C., Stephenson, S.R. 2013. New Trans-Arctic shipping routes navigable by mid-century. *Proceedings of the National Academy of Sciences U.S.A.*, 110 (13): E1191 – E1195, doi: 10.1073/pnas.1214212110.

Statistics Canada. 2013. Igloolik, Nunavut. Aborigional Population Profile. http:// www12.statcan.ca/census-recensement/2006/dp-pd/prof/92-594/index.cfm?Lang=E (accessed March 7, 2015).

Statistics of Greenland. 2013. Greenland in Figures 2013. http://www.stat.gl/dialog/main.asp?lang=en&sc=GF&version=2013 (accessed March 7, 2015).

Stieglitz, M., Déry, S.J., romanovsky, V.E., Osterkamp, T.E. 2003. The role of snow cover in the warming of the arctic permafrost. *Geophysical Research Letters*, 30 (13): 1721, doi: 10.1029/2003GL017337.

Stow, D.A., Hope, A., McGuire, D. et al. (2004) Remote sensing of vegetation and land-cover change in Arctic Tundra Ecosystems. *Remote Sensing of Environment*, 89, 281–308.

Streletskiy, D.A., Shiklomanov N.I., Nelson F.E. 2012a. Permafrost, infrastructure and climate change: A GIS-based landscape approach to geotechnical modeling. Arctic, *Antarctic and Alpine Research*, 44(3), 368-380. DOI: 10.1657/1938-4246-44.3.368.

Streletskiy, D.A., Shiklomanov N.I., Hatleberg E. 2012b. Infrastructure and a Changing Climate in the Russian Arctic: A Geographic Impact Assessment. *Proceedings of the 10th International Conference on Permafrost*, Salekhard, Russia, June 25 - 29, 2012, Vol.1, 407-412.

Streletskiy, D.A., Tananaev, N.I., Opel, T., Shiklomanov, N.I., Nyland, K.E., Streletskaya, I.D., Tokarev, I., Shiklomanov, A.I. 2015. Permafrost Hydrology in Changing Climatic Conditions: Interannual variability of stable isotope composition in rivers indicate role of permafrost degradation. *Environmental Research Letters*, In Review.

Sturm, M., Schimel, J.P., Michaelson, G.J., Welker, J.M., Oberbauer, S.F., Liston, G.E., Fahnestock, J.T., Romanovsky, V.E. 2005. Winter Biological Processes Could Help Convert Arctic Tundra to Shrubland. *BioScience*, 55: 12 – 26.

Tape, K., M. Sturm, and C. Racine. 2006. The evidence for shrub expansion in northern Alaska and the pan-Arctic. *Global Change Biology* 12:686–702.

Tchebakova, N.M., Parfenova, E., Soja, A.J. 2009. The effects of climate, permafrost and fire on vegetation change in Siberia in a changing climate. *Environmental Research Letters*, 4: 045013.

Todd, W.J. 1977. Urban and regional land use change detected by using Landsat data. *Journal of Research*, 5: 529-534.

Tømmervik, H., Johansen, B.E., Pedersen, J.P. 1995. Monitoring the effects of air pollution of terrestrial ecosystems in Varanger (Norway) and Nikel-Pechenga (Russia) using remote sensing. In: D.H. Landers, S.J. Christie (eds.). Ecological

effects of Arctic airborne contaminants. *Science of the Total Environment*, 160/161: 753 – 767.

US Census Bureau. 2015. State & county Quickfacts: North Slope Borough, A.K. http://quickfacts.census.gov (accessed March 7, 2015).

Vlasova, T.M., Kovalev, B.I., Filipchuk, A.N. 1992. Effects of point source atmospheric pollution on boreal-forest vegetation of northwestern Siberia. *National Park Service*, Anchorage, AK, USA, No. AD-P=007320/5/XAB.

Walck, J.L., Hidayati, S.N., Dixon, K.W., Thompson, K.E.N., Poschlod, P. 2011. Climate change and plant regeneration from seed. *Global Change Biology*, 17 (6), 2145 – 2161.

Walker, D.A., Jia, G.J., Epstein, H.E., Raynolds, M.K., Chapin, F.S., III, Copass, D.S., Hinzman, L.D., Kane, D., Maier, H., Michaelson, G.J., Nelson, F., Ping, C.L., Romanovsky, V.E., Shiklomanov, N., Shur, Y. 2003. Vegetation-soil-thaw-depth relationships along a Low-Arctic bioclimatic gradient, Alaska: Synthesis of information from the ATLAS studies. *Permafrost and Periglacial Processes*, 14: 103 – 123.

Walker, D.A., Forbes, B.C., Leibman, M.O., Epstein, H.E., Bhatt, U.S., Comiso, J.C., Drozdov, D.S., ... Yu, Q. 2011. Cumulative Effects of Rapid Land-Cover and Land-Use changes on the Yamal Peninsula, Russia. In *Eurasian Arctic Land Cover and Land Use in a Changing Climate*, pg. 207-236. Springer, Netherlands.

Walker, D.A., Leibman, M.O., Epstein, H.E., Forbes, B.C., Bhatt, U.S., Raynolds, M.K., Comiso, J.C., … Yu, Q. 2009. Spatial and temporal patterns of greenness on the Yamal Peninsula, Russia: interactions of ecological and social factors affecting the Arctic normalized vegetation index. *Environmental Research Letters*, 4: 045004. doi:10.1088/1748-9326/4/4/045004.

Walker, D.A., Webber, P.J., Binnian, E.F., Everett, K.R., Lederer, N.D., Nordstrand, E.A., Walker, M.D. 1987. Cumulative Impacts of Oil Fields on Northern Alaskan Landscapes. *Science*, 238 (4828): 757-761.

Wallace, J. S. 2012. *Using Landsat Imagery to Evaluate Landscape-level Impacts of Natural Gas Field Development: Tazovsky Peninsula, Russia, 1984-2007* (Master's thesis). The University of Montana, Missoula.

Walter, D., Heue, K.P., Rauthe-Schöch, A., Brenninkmeijer, C.A.M., Lamsal, L.N. 2012. Flux calculation using CARIBIC DOAS aircraft measurements: SO_2 emission of Norilsk. *Journal of Geophysical Research*, 117: D11305, doi: 10.1029/2011JD017335.

Webber, B. 2014. ‘Government close to the people’: on decentralization in Nunavut. *Polar Geography*, 37 (2): 177 – 192.

Williams, P., Smith, M. 1989. *The Frozen Earth*. Cambridge University Press, Cambridge, UK.

Yershov, E.D., Kondrat’yeva, K.A., Loginov, V.F., I.K. Sychev. 1996. Geocryological map of the USSR. *Faculty of Geology, Lomonosov Moscow University, and Russian Ministry of Geology* (Trans., 16 sheets, scale 1:2 500 000), Moscow, Russia. (Origional work published 1991).

Yoshikawa, K., Hinzman, L.D. 2003. Shrinking thermokarst ponds and ground water dynamics in discontinuous permafrost near Council, Alaska. *Permafrost and Periglacial Processes*, 2003, 14: 151 – 160.

Zellen, B. 2009. *On thin ice: The Inuit, the state and the challenge of Arctic sovereignty*. Latham: Lexington Books.

Zubareva, O.N., Skripal’shchikova, L.N., Greshilova, N.V., Kharuk, V.I. 2003. Zoning of landscapes exposed to technogenic emissions from the Norilsk mining and smelting works. *Russian Journal of Ecology*, 34: 375 – 380.